Brodogradnja Volume 77 Number 2 (2026) 77204

University of Zagreb Faculty of Mechanical Engineering and Naval Architecture

journal homepage: www.brodogradnja.fsb.hr

Brodogradnja

An International Journal of Naval Architecture and Ocean Engineering for Research and Development

Development of collision-case-based testing scenarios for validating autonomous ship collision-avoidance algorithms

Jae-Yong Lee[1], *Ho Namgung*[2, *], *Joo-Sung Kim*[3]

[1]*Department of Maritime Transportation System, Mokpo National Maritime University, Mokpo 58628, Republic of Korea*
[2]*Department of Maritime Industry Convergence, Mokpo National Maritime University, Mokpo 58628, Republic of Korea*
[3]*Division of Navigation Science, Mokpo National Maritime University, Mokpo 58628, Republic of Korea*

ARTICLE INFO

Keywords:
Collision-avoidance
Autonomous ship
Testing scenarios
Actual collision
Trajectory extraction

ABSTRACT

The criticality of collision-avoidance technology for ensuring safe navigation of autonomous ships necessitates diverse testing scenarios that reflect complex maritime environments. However, previous testing scenarios, often based on virtual trajectories or simplified encounters, have shown limitations in adequately representing real-world conditions. This study proposes a novel framework for developing collision-avoidance testing scenarios based on actual collision cases. The framework consists of three stages: collision case collection, trajectory extraction, and scenario development. Relevant data were extracted from selected cases, and the trajectories of ships influencing the collision were combined to reconstruct the circumstances at the time of the incident. Encounter situations were then diversified by altering the roles and positions of own and target ships, and finally systematically categorised into a structured testing set. Unlike previous testing scenarios, the developed scenarios exhibit distinctive characteristics derived from actual collision cases, including situations where navigation rules cannot be strictly applied, dynamic encounters, speed variations, and environmental conditions. By reflecting real maritime environments, these scenarios provide a solid basis for validating and improving collision-avoidance algorithms. The proposed framework is expected to contribute not only to the advancement of autonomous-ship technology but also to the enhancement of maritime safety.

1. Introduction

Autonomous ships are innovative technologies that have garnered significant attention owing to their ability to autonomously perform complex decision-making processes, such as collision-avoidance and emergency response, resulting in human-error reduction and maritime-accident minimisation [1]. Accordingly, based on the International Regulations for Preventing Collisions at Sea (COLREGs) [2], various collision-avoidance algorithms, developed by applying robotics and machine learning techniques, have been established as a core technology for commercialising autonomous ships [3].

* Corresponding author.
E-mail address: ngh2009@mmu.ac.kr

https://doi.org/10.21278/brod77204
Received 5 August 2025; Received in revised form 1 October 2025; Accepted 18 October 2025
Available online 29 October 2025
ISSN 0007-215X; eISSN 1845-5859

Collision-avoidance algorithms support automated decision-making in complex maritime environments. Therefore, comprehensive validation through realistic and diverse maritime scenarios is essential to ensure their safety and adaptability [4-6]. Among these, port environments pose unique challenges owing to limited manoeuvring space, high traffic density, and dynamic vessel movements, making it crucial to evaluate collision-avoidance algorithms using port-specific scenarios that incorporate various real-world factors, such as weather conditions, non-compliant ships, and complex situations that cannot be resolved solely through navigational rules [7].

Previous testing scenarios can be broadly categorised into three types based on data sources: 1) rule-based, 2) randomly generation, and 3) trajectory extraction [8].

Rule-based scenarios are virtual reconstructions of navigation techniques and challenges encountered by navigators in real-world maritime environments, and they are designed based on navigational rules such as COLREGs. These scenarios have been used in ship-handling simulation trainings to help navigators develop the skills needed to respond appropriately to complex real-world situations [9]. A representative example is the Imazu problem [10]. The Imazu problem consists of 22 basic scenarios, ranging from simple situations involving two ships to more complex situations involving up to four ships and 20 additional complex scenarios. Subsequently, Wang et al. [11, 12] proposed 54 extended scenarios based on the Imazu problem. Sawada et al. [13] implemented a new set of scenarios by leveraging COLREGs and encounter angle characteristics. They also expanded two-ship encounter situations into three-ship encounters through scenario combinations. Chen et al. [14] proposed a combinatorial-testing-based scenario generation method that optimises spatial and temporal complexity, enabling the creation of diverse and non-trivial encounter cases for collision-avoidance algorithm evaluation.

Randomly generated scenarios are created by generating diverse situations based on specific rules or conditions without relying on particular experiences or data. This approach allows the extraction of scenarios that cover a wide range of situations. A representative example is the use of Monte Carlo simulations to generate scenarios [15]. Porres et al. [16] proposed a method for generating random scenarios using a random vector generation algorithm; they tested collision-avoidance algorithms for high-risk scenarios, which were identified through scenario risk prediction using deep neural networks. Torben et al. [17] modelled scenarios with random variables using a Gaussian process to test collision-avoidance algorithms. Bolbot et al. [18] used the Sobol sequence to automatically generate testing scenarios and constructed a set of testing scenarios through sampling and clustering techniques.

In trajectory-extraction-based scenarios, large volumes of trajectory data are collected from automatic identification system (AIS), and the scenarios are implemented by extracting AIS trajectories that meet specific conditions, such as traffic congestion areas or close-encounter situations [19]. Various AIS trajectory-based techniques for scenario development have been continuously advanced in recent years to test collision-avoidance algorithms for autonomous ships [8]. Bakdi et al. [20] used maritime traffic big data to design testbed scenarios that capture conflicts, collision/grounding risks, and spatio-temporal dependencies, enhancing the realism of autonomous ship trials. Zhu et al. [5] proposed a method for testing collision-avoidance algorithms using randomly generated scenarios based on actual AIS trajectory data.

Meanwhile, Hwang and Youn [4] proposed a method for developing graph-based modelling scenarios by extracting unit scenarios with collision risks from AIS trajectory data, converting them into vector forms, and utilising similarity matrices. Wang et al. [8] developed a scenario generation framework by extracting encounter situations through proximity analysis in the same spatiotemporal context from the large volumes of AIS trajectory data, along with scenario-importance evaluation and disproportionate-probability sampling. Additionally, in their testing methodology, Dai et al. [21] designed an autonomous ship testing platform by integrating virtual and real-world scenarios and specifying test areas that reflect the realistic navigation conditions and environments of ships. Recently, hybrid approaches that combine trajectory extraction methods with random generation techniques have been utilised to create more complex scenarios [5, 21]. In addition, learning-based scenario generation algorithms have been proposed to further improve testing effectiveness. Specifically, Zhu et al. [22] introduced a reinforcement-learning-based high-risk scenario generation method that adaptively constructs critical situations to expose the limitations of autonomous collision-avoidance decision-making systems.

While rule-based scenarios often conform to COLREGs, they have two significant limitations: a limited scope that cannot encompass all real-world encounter situations and an underlying assumption that all vessels comply with navigational rules, thereby excluding non-compliant vessel behaviours.

In contrast, randomly generated scenarios can theoretically include all possible encounter situations depending on the scale of the generation, and the number of scenarios can be infinitely expanded. However, they lack realism because they are not based on actual cases and do not provide information beyond the encounter situation.

Conversely, trajectory-extraction-based scenarios that use large-scale AIS trajectory data can provide a sufficient number of scenarios, reflecting real-world maritime encounters, thereby ensuring realism [5, 8]. However, owing to the use of only AIS trajectory data, they lack detailed information about external environments or navigational conditions at the time, such as weather conditions or circumstances on the route. This limitation also applies to both rule-based and randomly generated scenarios.

To address these differences, the structures, characteristics, and techniques used in the collision-avoidance testing scenarios were compared in detail for each study (Appendix 2). Previous studies did not consider actual collision cases, encounter types, or speed variations. Furthermore, none of the studies included in-port situations or considered environmental factors, except for Dai et al. [21], who incorporated a specific test area and integrated real-world navigational conditions.

As research continues to address emerging complexities such as target ship (TS) uncertainty [23] intricate inland waterways [24-26], and the anticipation of ship behaviours in multi-vessel scenarios [27, 28], the demand for testing scenarios that faithfully reflect these real-world conditions has become increasingly critical for reliable validation of collision-avoidance algorithms for autonomous ships [29-34]. This gap highlights the necessity for a new approach to scenario development that incorporates actual collision cases, environmental complexities, and port-specific conditions.

To address these issues, this study was aimed at developing collision-avoidance testing scenarios based on actual collision cases to evaluate the performance of collision-avoidance algorithms for autonomous ships. The proposed framework is not intended to replace testing methodologies under normal operating conditions, but rather to complement existing scenarios. In particular, the approach based on actual collision cases is important, as collisions occurred under specific encounter situations, which provides meaningful data for prioritizing the training of autonomous ship agents. Therefore, the outcomes of this study, when combined with previously developed scenarios, can contribute to a more comprehensive validation of collision-avoidance algorithm performance.

This paper is organised as follows: In Section 2, the theoretical background, including the determination of collision risks and identification of encounter types between ships, is introduced. In Section 3, the process of developing the test scenarios is described, along with the methodologies applied at each development stage. In Section 4, the results of the scenario development are presented and then analysed and compared with previous testing scenarios. Finally, in Section 5, the paper is concluded and directions for future research are mentioned.

2. Theoretical background

2.1 Identification of collision risks

2.1.1 Fuzzy inference system based on near-collision (FIS-NC)

A FIS-NC provides a quantitative and real-time method for assessing collision risk without being constrained by geometric shapes [35, 36]. To integrate AIS data, variables such as relative distance (D_r), distance at closest point of approach (D_{CPA}), time to closest point of approach (T_{CPA}), variation of compass degree (VCD) of the TS, were extracted. These variables were processed using an adaptive neuro-fuzzy inference system to train membership functions that subsequently compute the collision risk index (CRI) [36]. Parameters D_r, D_{CPA}, T_{CPA}, and VCD were obtained through geometric calculations (Fig. 1) and calculated using Eqs. (1)-(6):

$$D_r = \sqrt{(x_{ts} - x_{os})^2 + (y_{ts} - y_{os})^2} \tag{1}$$

$$V_r = V_{os} \times \sqrt{1 + (\frac{V_{ts}}{V_{os}})^2 - 2 \times \frac{V_{ts}}{V_{os}} \times cos(\varphi_{os} - \varphi_{ts})} \tag{2}$$

$$\varphi_r = cos^{-1}\left(\frac{V_{os} - V_{ts} \times cos(\varphi_{os} - \varphi_{ts})}{V_r}\right) \tag{3}$$

$$D_{CPA} = D_r \times sin(\varphi_r - \alpha_{ts} - \pi) \tag{4}$$

$$T_{CPA} = D_r \times \frac{cos(\varphi_r - \alpha_{ts} - \pi)}{V_r} \tag{5}$$

$$VCD_i = | \alpha_{r_i} - \alpha_{r_{i-1}} | \tag{6}$$

where V_{os} and V_{ts} denote the velocities of own ship (OS) and TS, respectively, and V_r represents relative velocity. φ_{os} and φ_{ts} represent the courses of OS and TS, respectively, and φ_r represents relative course. α_{ts} represents the true bearing of TS, and α_{r_i} represents the relative bearing with TS observed at time step i. The overall collision risk inference process in the FIS-NC framework is illustrated in Fig. 2 [36].

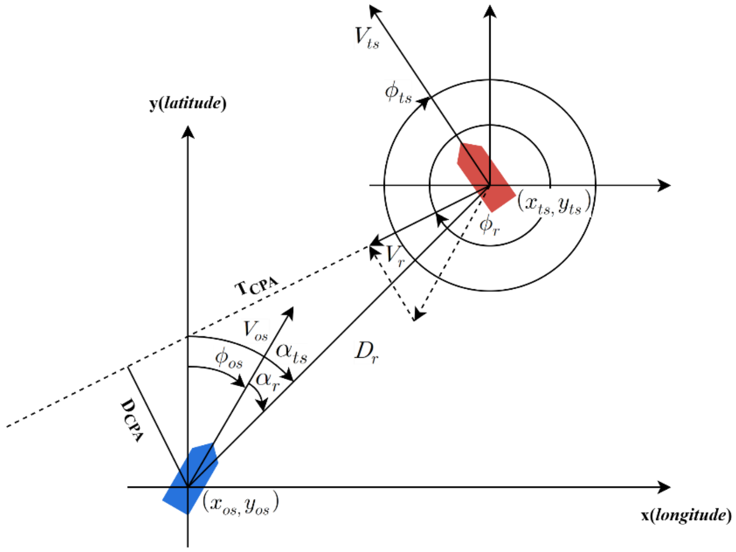

Fig. 1 Geometry collision of moving ship (T_{CPA}: Time to closest point of approach; D_{CPA}: Distance at closest point of approach)

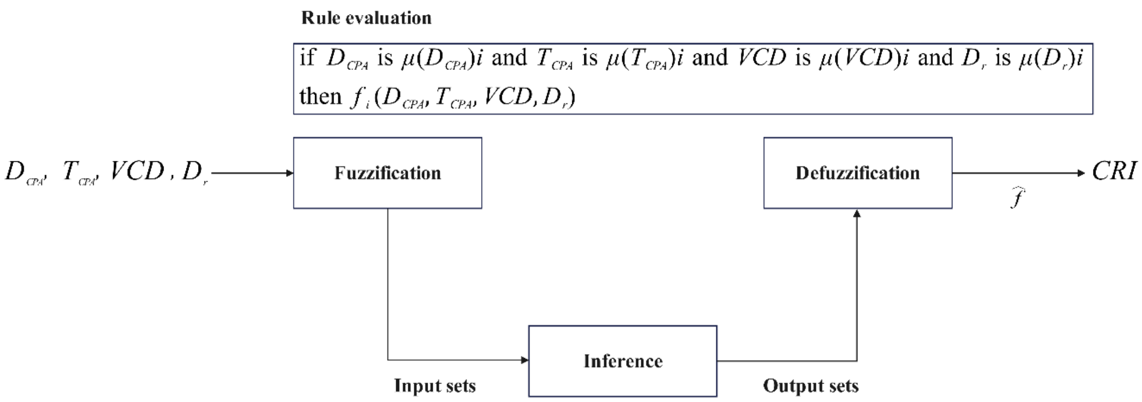

Fig. 2 Inference process of the fuzzy inference system based on near-collision (FIS-NC) (CRI: Collision risk index; VCD: Variation of compass degree)

The calculated CRI ranged from 0 to 1, and the CRI was segmented into distinct risk levels based on the stage of the collision-avoidance manoeuvres. The derivation for functions not discussed in this work can be found in the study by Namgung and Kim [36]. The corresponding CRI ranges for each risk level are listed in Table 1 [36].

Table 1 Range of CRI by level

	Attention	**Threat**	**Danger**	**Collision**
$\boldsymbol{CRI}$	$0.01 \leqq CRI < 0.33$	$0.33 \leqq CRI < 0.66$	$0.66 \leqq CRI < 1.00$	1.00

Namgung and Kim [36] defined CRI thresholds (0.01, 0.33, 0.66, 1.00) for each risk level based on the response distances (3, 2, 1, 0.25 miles) specified in COLREGs and near-collision data. These thresholds reflect the timing of collision-avoidance actions required by the give-way and stand-on vessels.

2.1.2 Variable ship domain ($V - SD$)

The $V - SD$ is based on the elliptical ship domain (SD) proposed by Fujii and Tanaka [37]. The elliptical SD (Fig. 3) can be calculated using Eqs. (7) and (9) [36, 37].

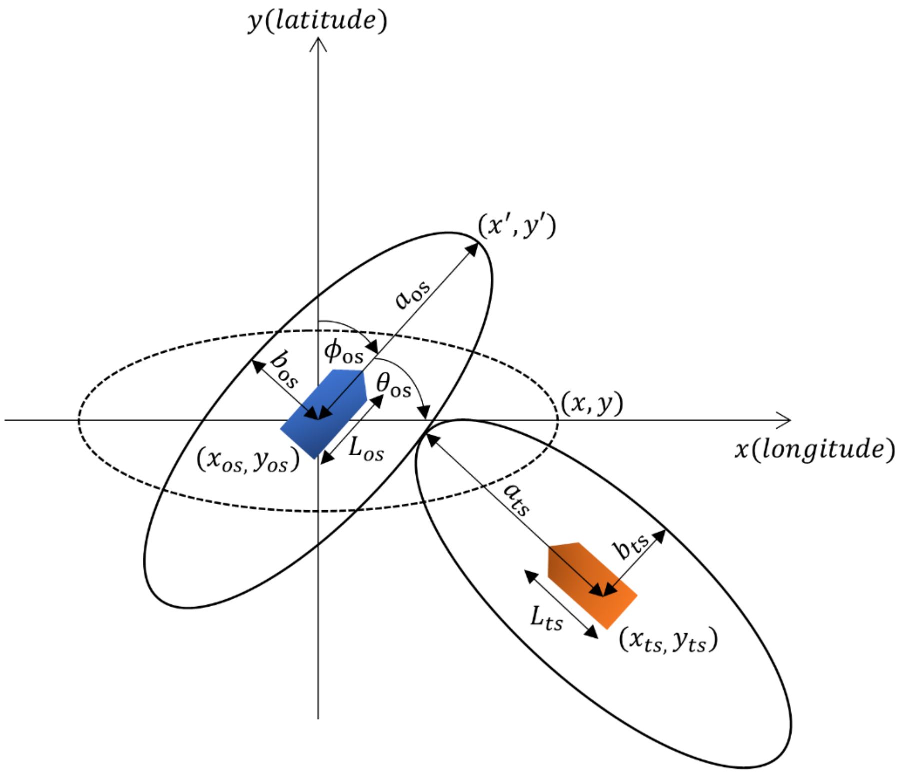

Fig. 3 SD with elliptical dimension

In the figure, L_{os} represents the length of the OS; a_{os} and b_{os} denote the semi-major and semi-minor axes, respectively. The SD, rotated in the direction of the course of the ship, can be calculated as:

$$\frac{(x' - x_{os})^2}{(a_{os} \times L_{os})^2} + \frac{(y' - y_{os})^2}{(b_{os} \times L_{os})^2} = 1 \tag{7}$$

The $V - SD$ size varies depending on the velocity, ranging from $2L_{os} \times 0.4L_{os}$ to $8L_{os} \times 3.2L_{os}$. For every 0.1 change in velocity, the semi-major axis (a_{os}) and semi-minor axis (b_{os}) of the OS can be determined using Eqs. (8) and (9), respectively [36]:

$$a_{os} = \begin{cases} \dfrac{8L_{os} - \left(\dfrac{(V_{10\,kn} - V_{os}) \times 0.06}{0.1\,kn}\right)}{2} & if\ (V_{os} \le V_{10\,kn}) \\ \dfrac{8L_{os} + \left(\dfrac{(V_{os} - V_{10\,kn}) \times 0.06}{0.1\,kn}\right)}{2} & if\ (V_{os} > V_{10\,kn}) \end{cases} \tag{8}$$

$$b_{os} = \begin{cases} \dfrac{3.2L_{os} - \left(\dfrac{(V_{10\,kn} - V_{os}) \times 0.028}{0.1\,kn}\right)}{2} & if\ (V_{os} \le V_{10\,kn}) \\ \dfrac{3.2L_{os} + \left(\dfrac{(V_{os} - V_{10\,kn}) \times 0.028}{0.1\,kn}\right)}{2} & if\ (V_{os} > V_{10\,kn}) \end{cases} \tag{9}$$

Namgung and Kim [36] proposed 10 kn as a reference velocity for the $V - SD$ scaling, as both the static model by Fujii and Tanaka [37] and the adaptive model by Bakdi et al. [38] yield similar SD dimensions at this speed ($a = 4L$, $b = 2.25L$). This convergence justifies the use of 10 kn as a baseline, around which the $V - SD$ is dynamically adjusted using quadratic expressions to reflect changes in ship manoeuvrability. Here, $V_{10\,\mathrm{kn}}$ represents the velocity in 10 kn. The semi-major axis (a_{ts}) and semi-minor axis (b_{ts}) of the TS can be determined by substituting corresponding values of the TS (L_{ts}, V_{ts}) into Eqs. (8) and (9), respectively.

2.2 Identification of encounter situation between ships

Namgung [39] classified sectors based on the course of OS (φ_{os}) and relative bearing (α_r). They used the encounter angle (φ_e)—the angle at which φ_{os} intersects with the course of TS (φ_{ts})—to determine the encounter type between ships. The α_r and φ_e can be geometrically depicted as in Fig. 4. The φ_e can be calculated using Eq. (10); if the result is negative, 2π is added [39]:

$$\varphi_e = \varphi_{ts} - \varphi_{os} - \pi \tag{10}$$

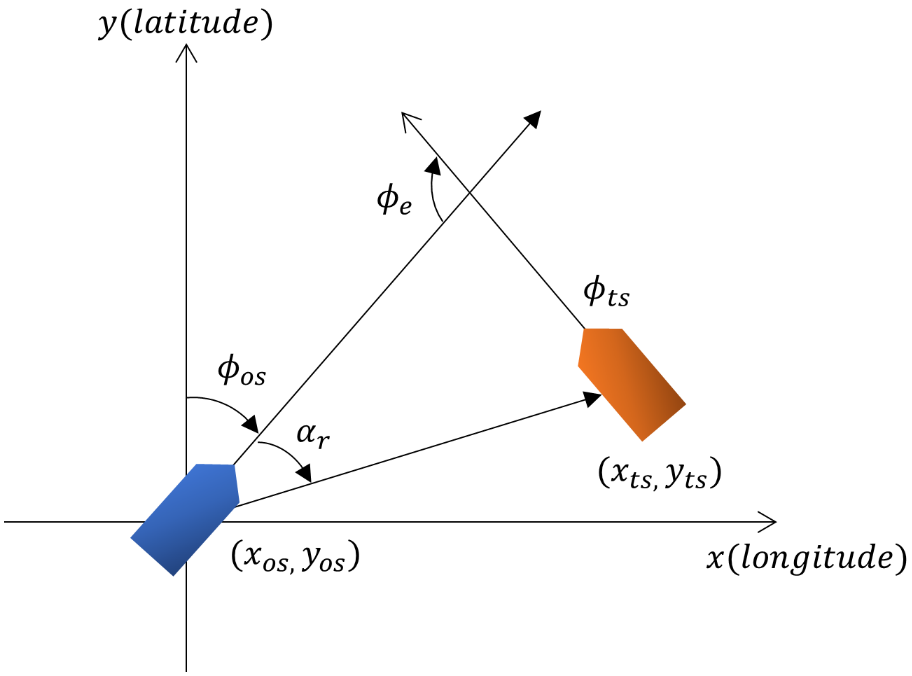

Fig. 4 Relative bearing and encounter angle

In this approach, the sector was divided into six regions, and the encounter types were classified into eight categories according to COLREGs: head on, crossing give-way, crossing quarter-lee give-way, crossing stand-on, crossing quarter-lee stand-on, overtaking, being overtaken, and safe. The range of head on motion was defined as 348.75° to 11.25°. The encounter type table developed by Namgung [39] is shown in Fig. 5.

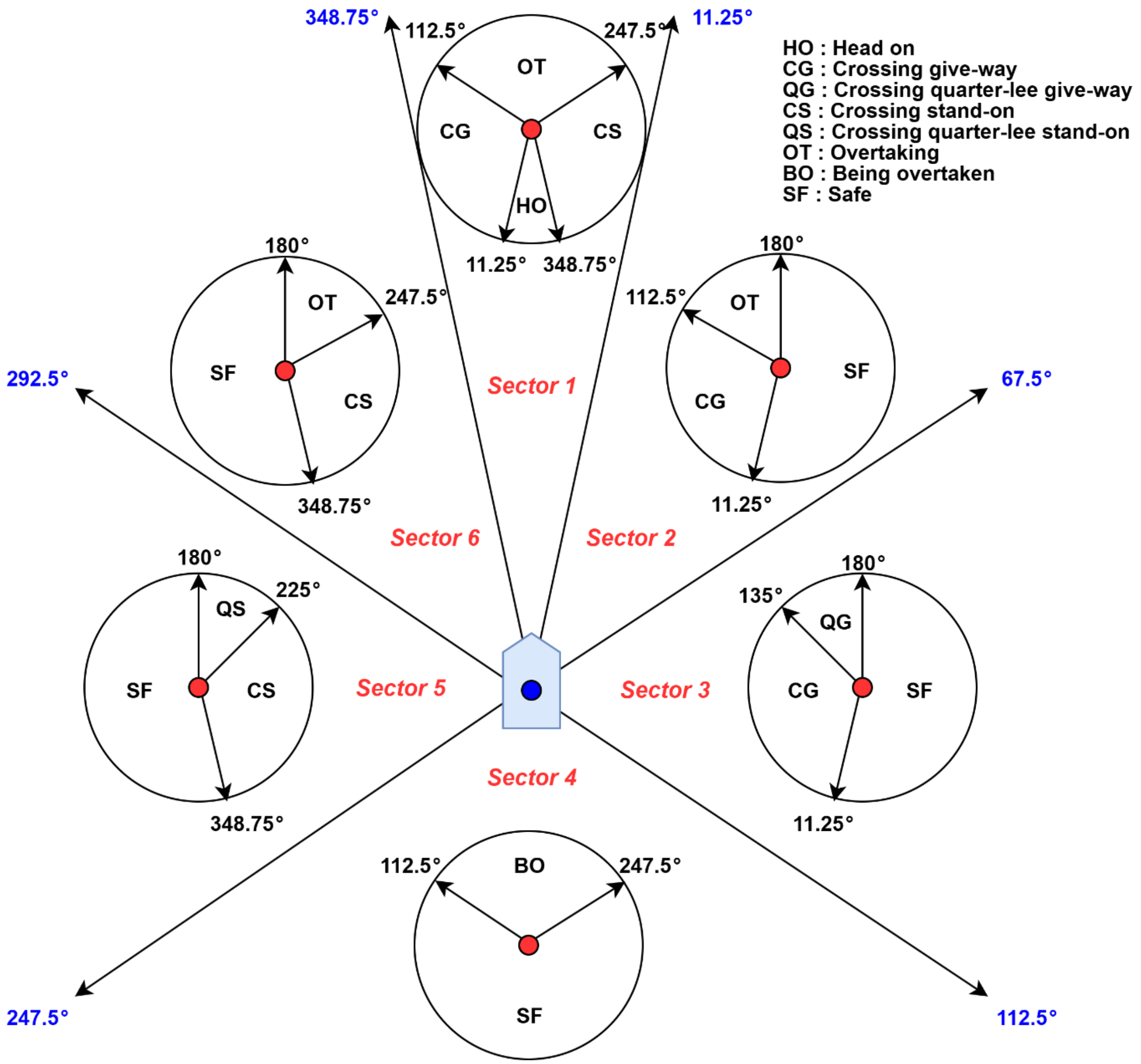

Fig. 5 Encounter type table

The angles dividing the sectors are 11.25°, 67.5°, 112.5°, 247.5°, 292.5°, and 348.75°. The circles within each sector represent TS, and the encounter type of the OS can be determined through the φ_e within these circles. Depending on the encounter type, the avoidance manoeuvers of the owners varied.

3. Actual-collision-case-based scenario development

3.1 Scenario development framework

The testing-scenario development framework proposed in this study is illustrated in Fig. 6. It comprised of three stages: collision case collection, trajectory extraction, and scenario development.

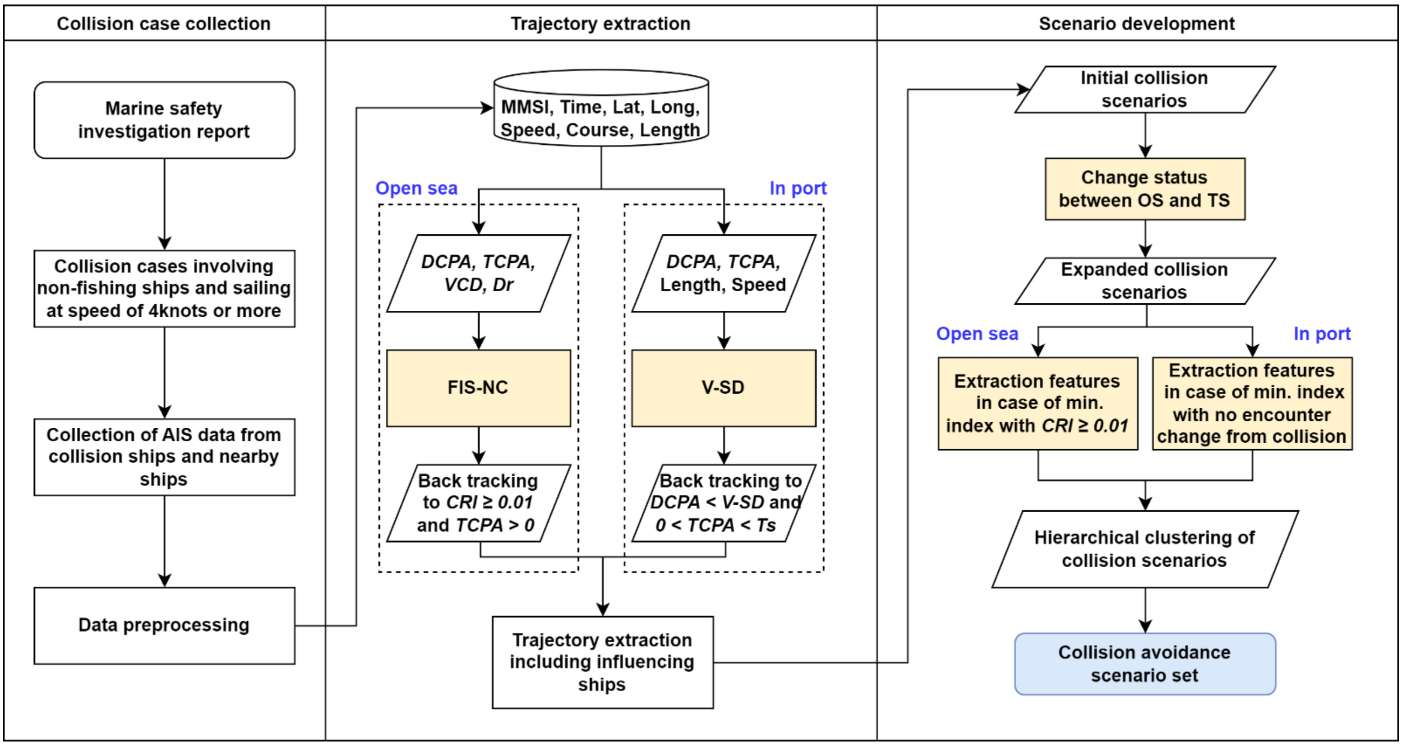

Fig. 6 Framework of development of testing scenario

First, in the collision case collection stage, actual collision cases relevant to the study were selected and the corresponding data were collected. Subsequently, in the trajectory extraction stage, the trajectories of the colliding ships were identified; other vessels whose movements may have influenced the decision-making of the colliding ships were also identified. The identification of ships affecting the collision was based on different approaches depending on the location: 1) in open waters, FIS-NC [36] was employed, and 2) within port limits, the $V-SD$ [36] was used. Finally, in the scenario development stage, new collision scenarios were generated by altering the roles of the OS and TS to examine the decision-making processes of the TS and obtain various encounter situations. Then, the characteristics of each collision scenario were extracted, and hierarchical clustering was applied to group similar encounter situations and systematically structure the scenarios.

3.2 Investigation of collision accident cases

3.2.1 Selection of collision accident cases

Collision accident cases were selected based on marine accident investigation reports and collision location data provided by the Korean maritime safety tribunal (KMST) [40, 41] (Fig. 7). Cases were excluded if the AIS trajectory information was inaccurate or irregular owing to fishing operations or recreational activities. Additionally, collision cases involving non-navigating (anchored or adrift) ships were excluded owing to the study objectives.

The speed criterion for navigating ships was set to a minimum of 4 kn, as defined by the International Maritime Organisation (IMO), which represents the minimum speed required to maintain manoeuvrability, including rudder effectiveness, under adverse conditions [42]. The selection criteria for the collision cases are listed in Table 2.

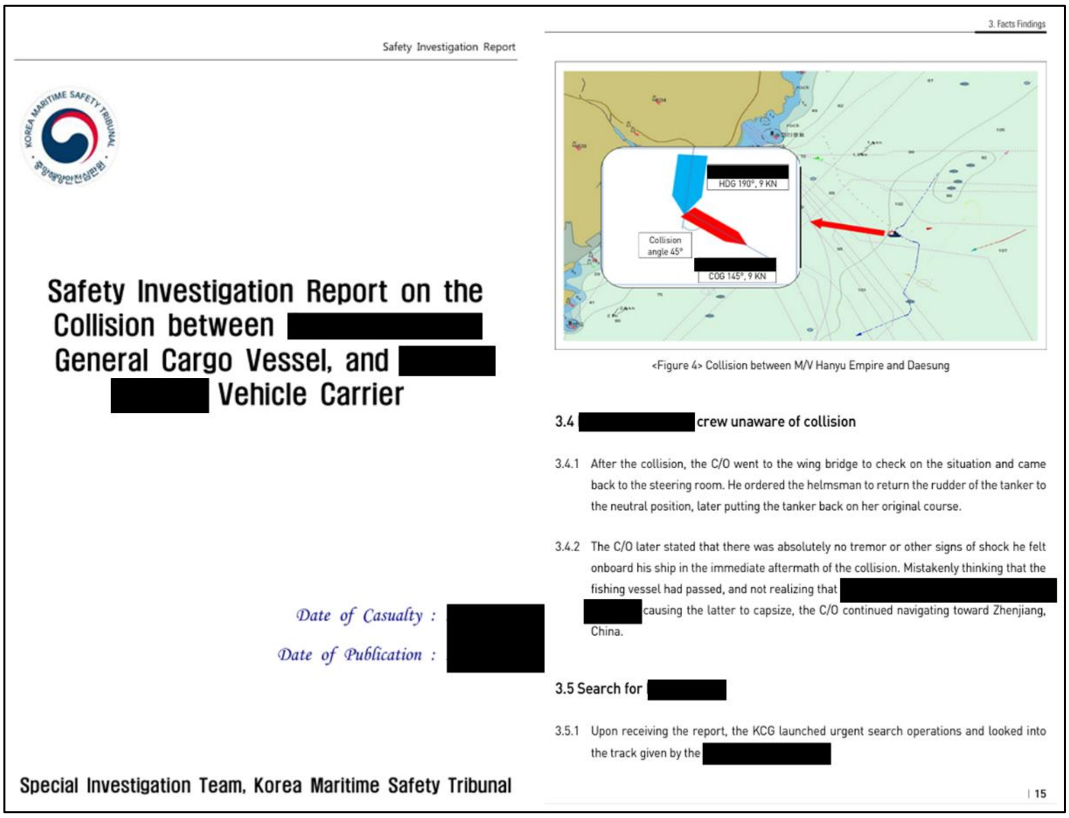
Safety Investigation Report

Safety Investigation Report on the Collision between [redacted] General Cargo Vessel, and [redacted] Vehicle Carrier

Date of Casualty : [redacted]
Date of Publication :

Special Investigation Team, Korea Maritime Safety Tribunal

3. Facts Findings

<Figure 4> Collision between M/V Hanyu Empire and Daesung

3.4 [redacted] crew unaware of collision

3.4.1 After the collision, the C/O went to the wing bridge to check on the situation and came back to the steering room. He ordered the helmsman to return the rudder of the tanker to the neutral position, later putting the tanker back on her original course.

3.4.2 The C/O later stated that there was absolutely no tremor or other signs of shock he felt onboard his ship in the immediate aftermath of the collision. Mistakenly thinking that the fishing vessel had passed, and not realizing that [redacted] causing the latter to capsize, the C/O continued navigating toward Zhenjiang, China.

3.5 Search for [redacted]

3.5.1 Upon receiving the report, the KCG launched urgent search operations and looked into the track given by the [redacted]

| 15

Fig. 7 Safety investigation report by KMST

Table 2 Criteria for target accidents

No.	Criteria	Description
1	Period	In the last 5 y ('19–'23)
2	Boundary	In South korean waters (Inc. EEZ)
3	Type of TS	Non-fishing, Non-pleasure craft
4	Speed of TS	Over 4 kn (status of underway)

(EEZ: Exclusive economic zone)

A total of 19 collision cases meeting these criteria were selected, including 12 cases in the open sea and seven cases in the port. Selected collision cases are shown in Fig. 8. The red and blue lines in the figure show the trajectories of the two colliding ships, with the blue line representing the ship of greater gross tonnage than the red one.

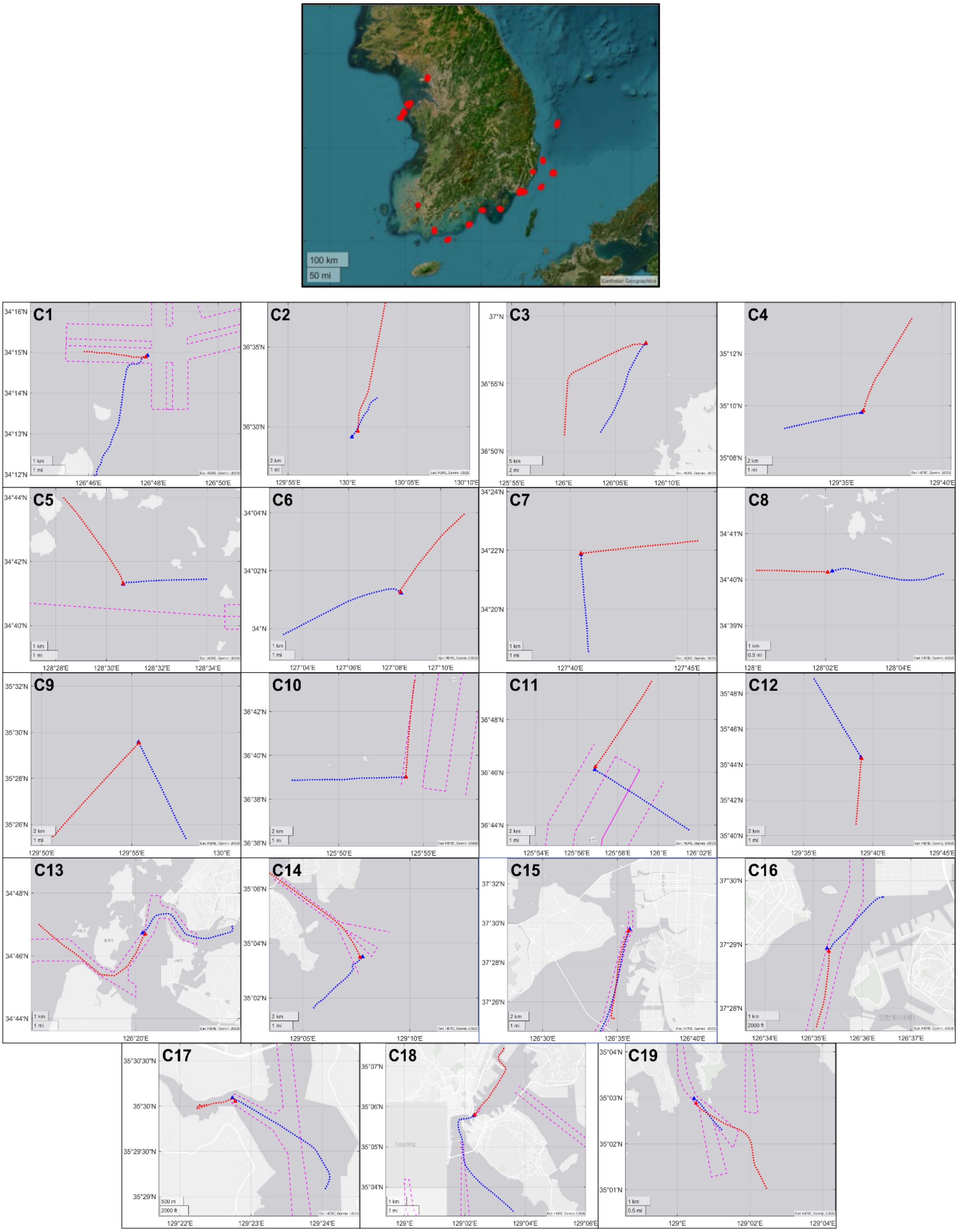

Fig. 8 Selected collision accident cases (C: Case)

3.2.2 Collection and analysis of collision accident data

For the selected cases, key factors potentially influencing accidents were collected (Table 3) based on marine accident investigation reports, collision data, and weather conditions at the time of the accidents. These factors included the visibility, wind, current, wave height, weather, ship type, ship length, and whether the ship is within a fairway. Diverse weather conditions were identified, such as strong winds and high waves (C6 and C12), restricted visibility (C12), and a strong current of 4.5 kn (C15). Additionally, the collision cases involved various ship types and sizes, ranging from an 11-m tugboat to a 347-m cruise ship. The dataset also included collisions occurring in a traffic separation scheme (TSS) (C1, C10, and C11) and fairways (C13–C19). In the port cases, speed restrictions ranging from 8 to 12 kn were applied (C13–C16, C18, and C19).

Table 3 Analysis of selected collision accident cases

Collision Location	Case	Visibility (nm)	Wind (dir./ms)	Current (dir./kn)	Wave (m)	Day/ Night	Weather	S1 (Length/m)	S2 (Length/m)	Fairway (inc. TSS)	Others
Open Sea	1	5	SE/6–9	281˚/0.7	1.0–1.5	Night	Cloudy	Passenger/40	Towing/25	✓	-
	2	3	SW/5–8	0	0.5	Day	Cloudy	Towing/11	General/90	-	-
	3	2	NW/5–7	052˚/1.1	1.0	Night	Cloudy	Bulk/287	Bulk/80	-	-
	4	6	NW/8–9	118˚/0.3	2.0	Night	Clear	Other/29.33	Tanker/176.20	-	-
	5	5	NW/4–6	264˚/0.2	0.5	Day	Clear	Tanker/35.05	Other/27.24	-	-
	6	7	NW/ 10–12	296˚/0.2	1.0–1.5	Night	Clear	Other/41.28	CNTR/119.4	-	-
	7	7	NW/6–8	321˚/0.3	0.5–1.0	Night	Clear	Other/39.91	General/94.79	-	-
	8	3	NE/4–5	264˚/0.7	0.5	Night	Clear	Tanker/39.38	Tanker/49.30	-	-
	9	5	NE/8–10	032˚/0.2	1.5	Night	Clear	Other/23.61	Tanker/146	-	-
	10	3	S/2–4	030˚/0.7	0.5	Day	Clear	Tanker/86.90	Other/30.83	✓	-
	11	5	NW/2–4	034˚/1.9	0.5	Night	Clear	Other/22.88	General/113.14	✓	-
	12	1	NW/ 10–12	204˚/0.2	2.0–3.0	Night	Cloudy	Other/21.93	General/75.03	-	-
In Port	13	2	NE/6–8	263˚/0.3	1.0	Night	Cloudy	RORO/140	Other/36	✓	Speed limit: 12 kn
	14	3	NW/3–4	218˚/0.6	0.5	Day	Clear	Towing/30.6	Cruise/347.7	✓	Speed limit: 10 kn
	15	3	NW/2–4	355˚/4.5	0.5	Night	Clear	Tanker/112.37	Towing/42.50	✓	Speed limit: 8 kn
	16	3	SW/4–6	032˚/1.3	0.5	Night	Clear	General/79.31	Towing/33.07	✓	Speed limit: 8 kn
	17	7	NE/4–8	0	0.5	Day	Clear	Tanker/79.99	Tanker/69.72	✓	-
	18	3	SW/6–8	044˚/0.5	0.5	Night	Clear	Tanker/29.38	Tanker/33.02	✓	Speed limit: 8 kn
	19	3	SW/2–3	345˚/0.1	0.5	Day	Clear	Towing/Barge 29.06(103.77)	General/97.77	✓	Speed limit: 10 kn

(TSS: Traffic separation scheme)

3.3 Extraction of actual collision accident trajectories

3.3.1 Collision scenario in open sea using FIS-NC

First, the AIS trajectories of the colliding ships were extracted along with those of all conventional ships navigating at speeds >4 kn [42] within a 4-mile radius of the collision point and time, based on the proximity encounter criteria in the guide to collision-avoidance rules [43]. Subsequently, for collision cases in the open sea, FIS-NC was employed to assess the collision risk in real time using quantitative values [35]. As defined by Eq. (11), ships with a CRI>0.01 (the attention stage when collision risk begins) and a T_{CPA}>0 were considered to influence a collision [36]:

$$CRI \geq 0.01 \quad and \quad T_{CPA} > 0 \tag{11}$$

Through this process, the ships that influenced the collisions were identified. The extraction process is illustrated in Fig. 9.

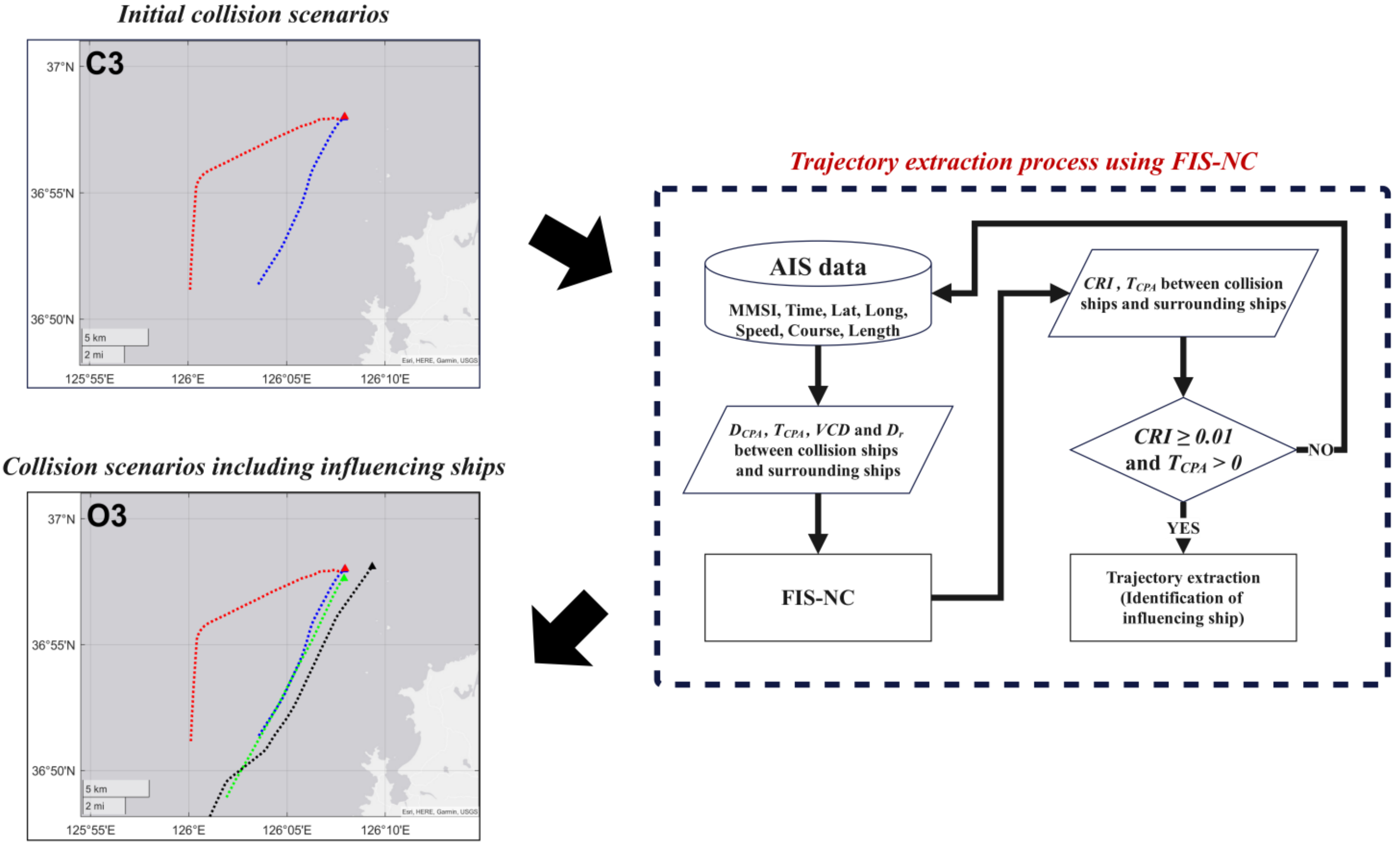

Fig. 9 Process of extracting influencing ships using FIS-NC

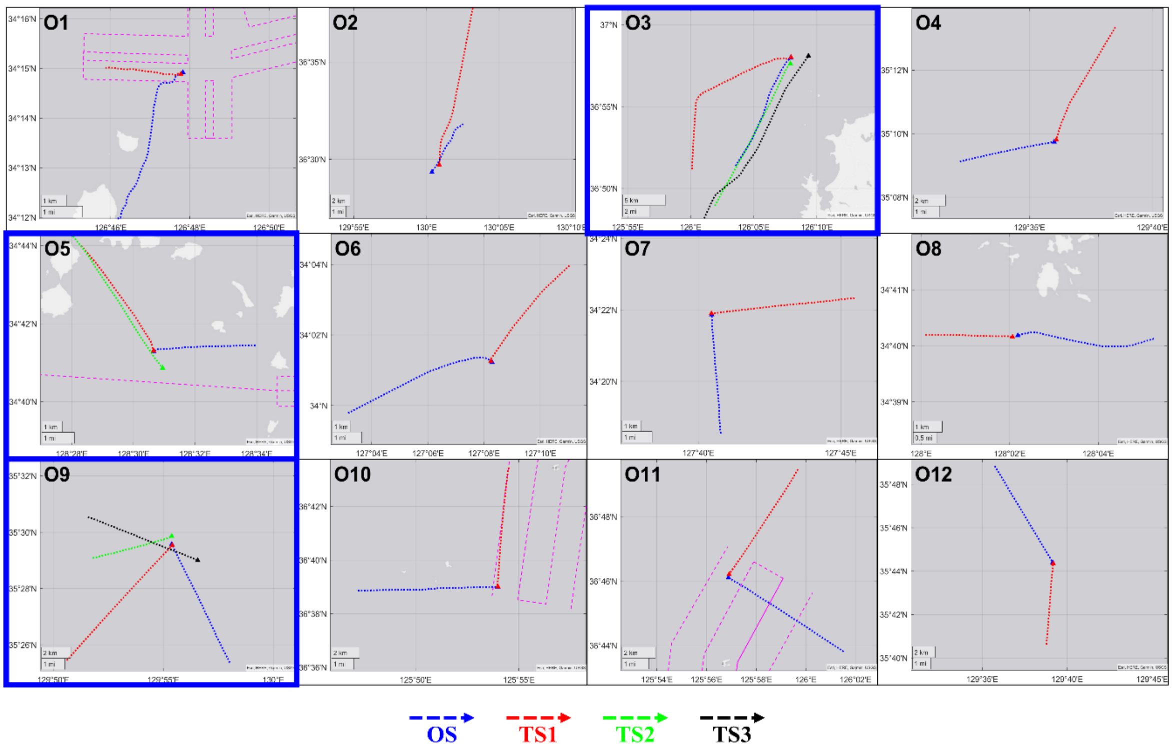

Fig. 10 Initial collision scenarios in open sea

The collision scenarios in the open sea included 12 cases (C1–C12) (Fig. 8). Among these, five ships with CRI>0.01, as identified by FIS-NC [36], were extracted as influencing ships in C3, C5, and C9. The trajectories of these ships were extracted, and these three cases were reclassified as multi-ship encounters. The collision scenarios in the open sea, including the trajectories of the influencing ships, are illustrated in Fig. 10. To distinguish between the collision scenarios in the open sea, scenario codes were assigned a combination of the letter O (open sea) and numbers.

Here, OS and TS1 represent the ships that collided with each other, whereas TS2 and TS3 are identified as ships that influenced the collision. Among the colliding ships, the OS was determined based on the priority order of ships involved in marine accidents as stipulated by the KMST, with the ship of greater gross tonnage designated as the OS [44].

3.3.2 Collision scenario in port using $V-SD$

The collision scenarios in ports consisted of seven cases (C13–C19) (Fig. 8). Considering the unique characteristics of collision scenarios in ports, where encounter types and speeds frequently change owing to external factors, such as routes and geography, the $V-SD$ was used instead of FIS-NC. The $V-SD$ allows intuitive judgment of collision risk in proximity and dynamically adjusts its size according to the speed of the ship [36]. Additionally, the incorporation of D_{CPA} and T_{CPA} as variables enabled a real-time collision risk assessment even of distant ships. As defined by Eq. (12), a ship was identified as influencing the collision if its D_{CPA} overlapped with the $V-SD$ of OS and its T_{CPA} was over 0 [45]:

$$D_{CPA} < V-SD_{os} \quad and \quad 0 < T_{CPA} < T_S \tag{12}$$

where $V-SD_{os}$ represents the major axis length of the $V-SD$ of OS. T_S was determined based on a speed limit of 12 kn [46] at Busan New Port, a representative smart port in South Korea where autonomous ships are expected to operate. This value corresponds to a collision time of 10 min for two ships travelling at 12 kn to meet at a distance of 4 miles, which is the proximity encounter criterion defined in the guide to collision-avoidance rules [43]. Additionally, situations with the collision risk persisting for a significant period, such as overtaking between ships with similar speeds, were considered to determine the time required to reach $V-SD_{os}$. T_S can be calculated as:

$$T_S = \begin{cases} \dfrac{V-SD_{os}}{V_r} & if\ \left(\dfrac{V-SD_{os}}{V_r} > 10\,min\right) \\ 10\,min & if\ \left(\dfrac{V-SD_{os}}{V_r} \le 10\,min\right) \end{cases} \tag{13}$$

Based on these criteria, the ships influencing the collision were identified, and their trajectories were extracted (Fig. 11).

Consequently, among the seven collision cases, six ships were identified as influencing the collisions in C2, C3, and C7, and their trajectories were extracted. These three cases, initially classified as 1:1 encounter, were reclassified as multi-ship encounters. To distinguish between the collision scenarios in ports, scenario codes combining the letter P (Port) and numbers were assigned. The collision scenarios at the port, including the trajectories of the influencing ships, are illustrated in Fig. 12.

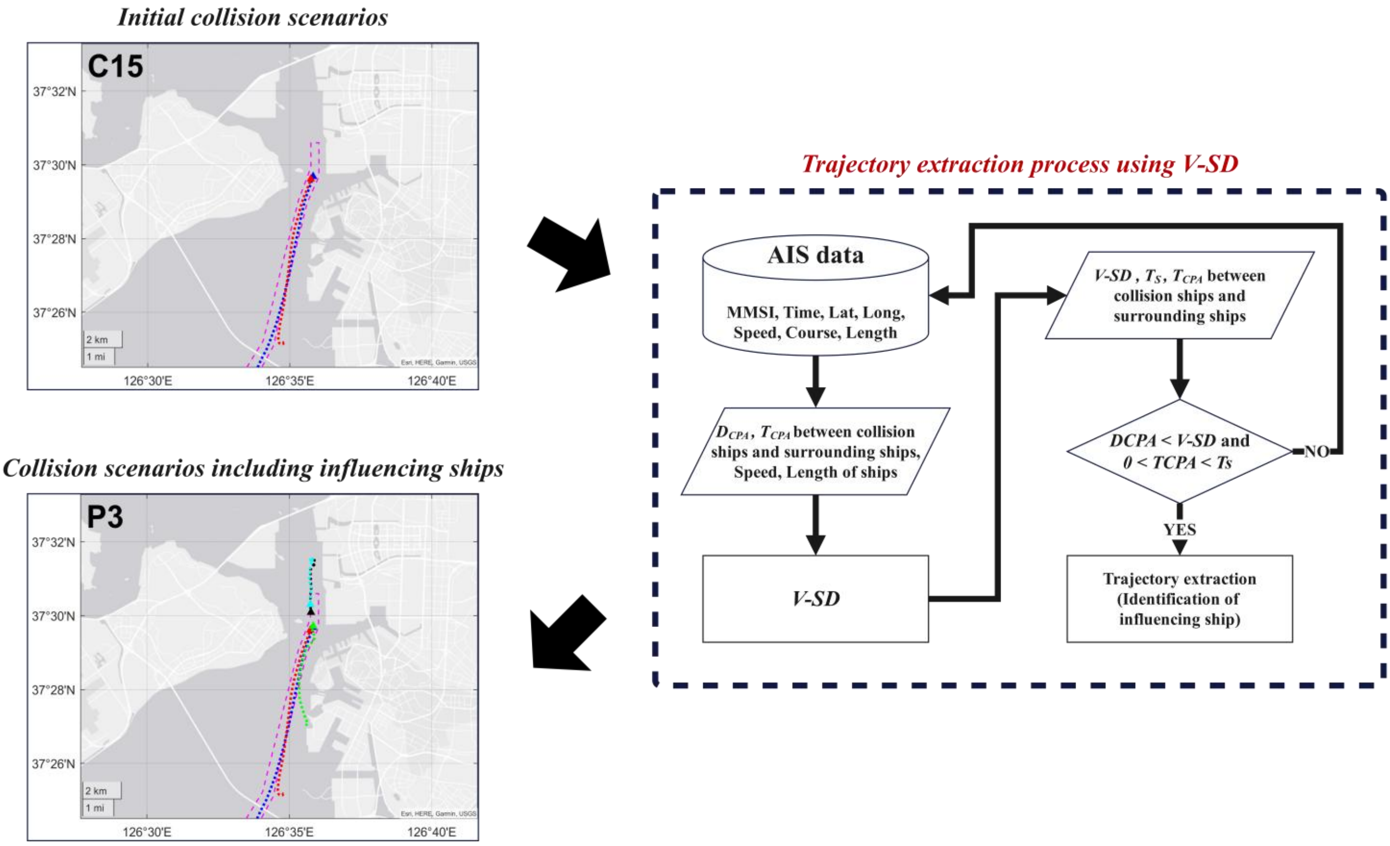

Fig. 11 Process of extracting influencing ships using $V-SD$

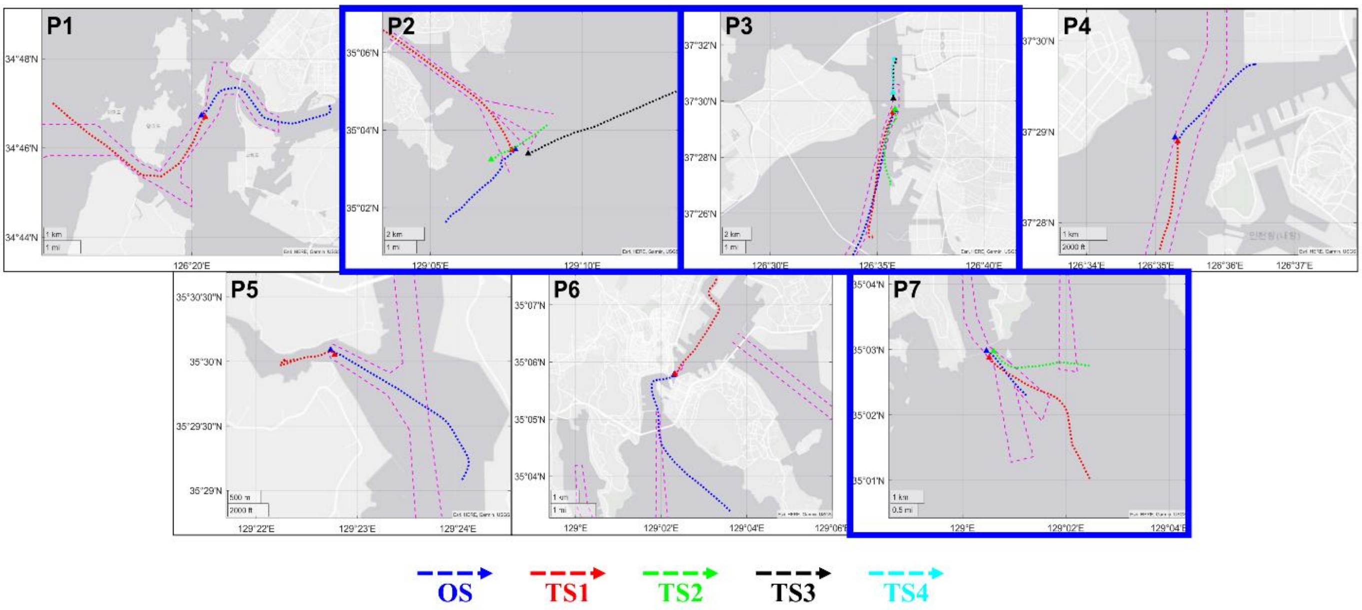

Fig. 12 Initial collision scenarios in port

The trajectory extraction algorithm including both collision ships and influencing ships is presented below.

Algorithm 1. Trajectory extraction

Input: Historical AIS data of actual collision cases [C1, C2, …, C19], AIS data (Latitude, Longitude) set = [C1(OS, TS1, …, TSn), C2(OS, TS1, …, TSn), …, C19(OS, TS1, …, TSn)]

Output: Set of initial collision scenarios including trajectories of collision ships and influencing ships. [O1(OS, TS1), O2(OS, TS1), O3(OS, TS1, TS2, TS3) …, P7(OS, TS1, TS2)]

% Extraction of initial trajectories
For each [C1, C2, …, C19]
IF AIS data are not from fishing ship
AND AIS data are not from leisure craft
AND it is sailing at 4 kn or more
THEN extract the trajectory of collision ships [OS, TS1]
IF there is ship within a 4-mile range from collision point(location and time)
AND the ship is neither a fishing ship nor a leisure craft
AND it is sailing at 4 kn or more
THEN extract the trajectory of all such ships [TS2, TS3, …, TSn]

% Extraction of trajectories influencing ships.
For each [TS2, TS3, …, TSn]
Distinguish between ‘open sea’ and ‘in port’ based on collision location.
IF collision case is in open sea
THEN calculate D_{CPA}, T_{CPA}, VCD, and D_r, with OS or TS1.
Calculate CRI using FIS-NC.
IF $T_{CPA} > 0$ AND $CRI \geq 0.01$ with OS or TS1
THEN identify influencing ship and extract its trajectory.
IF collision case is in port
THEN calculate D_{CPA}, T_{CPA} with OS or TS1.
Extract the ship length and speed of OS and TS1.
Calculate $V-SD$ for OS and TS1.
IF $D_{CPA} < V-SD$ AND $0 < T_{CPA} < T_S$ with OS or TS1
THEN identify influencing ship and extract its trajectory.
Construct a set of collision cases, involving collision and influencing ships.

3.4 Methodology for scenario development

3.4.1 Status change based on encounter relations

Testing scenarios must encompass diverse encounter situations. In multi-ship encounters, examining the decision-making processes among the TSs is essential. In this study, based on the 19 collision scenarios extracted through the trajectory extraction process, various encounter situations were created by altering the roles of the OS and TS (Fig. 13). Despite differences in the manoeuvring performance of OS and TS, the framework is based on AIS data rather than physical handling, thereby validating this role-swapping approach. This enabled an intuitive analysis of encounter situations from the perspective of the TS.

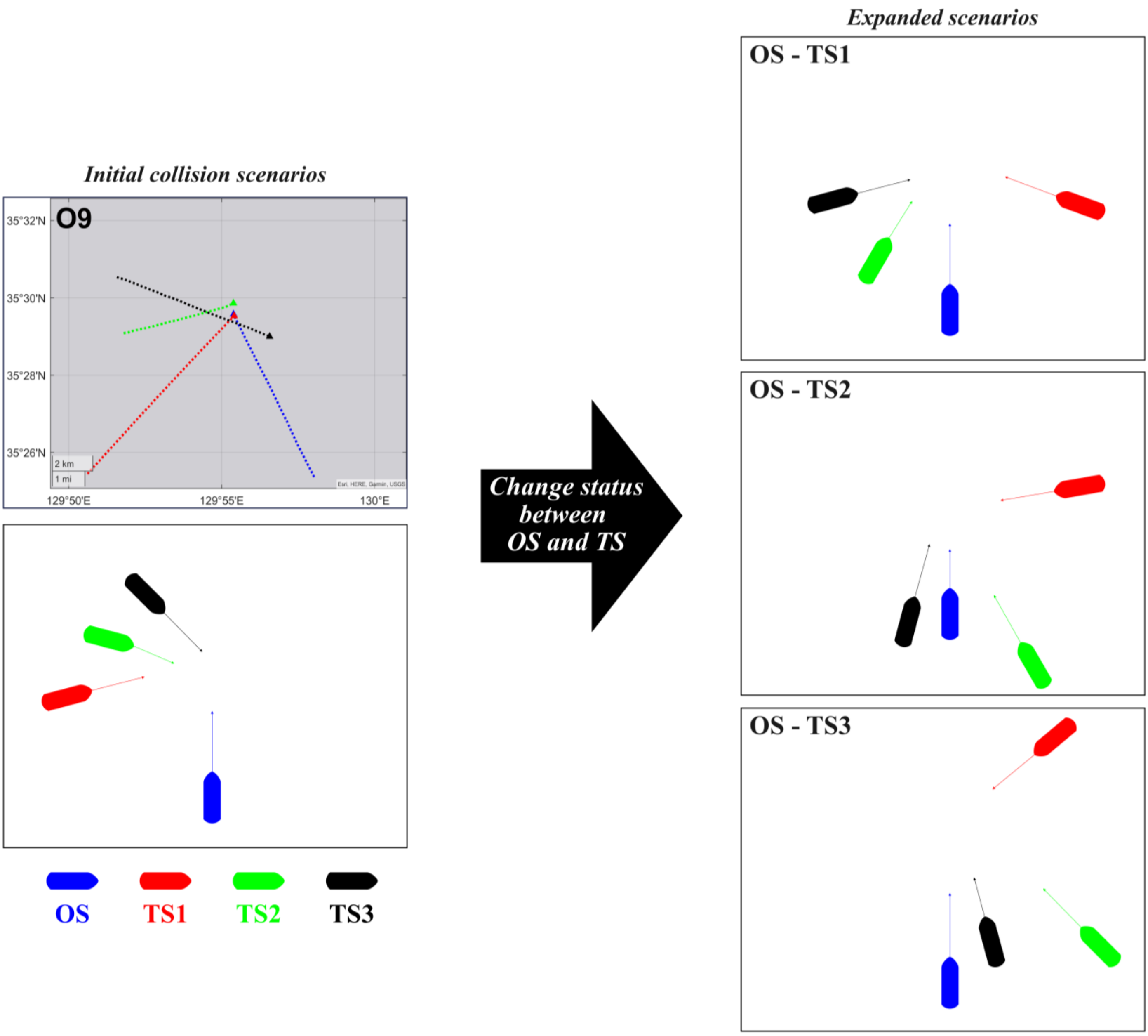

Fig. 13 Process of change status between OS and TS

3.4.2 Extraction of characteristics by collision scenarios

To extract the characteristics of each collision scenario for the cases in the open sea, the relative bearing and relative course data of the TSs were extracted based on the OS at the point when the FIS-NC-based CRI reached 0.01 [36], indicating the onset of collision risk.

Quantifying encounter situations is challenging. Therefore, text-based encounter characteristics, such as sector and encounter type, were extracted based on the relative bearing and relative course data of the TSs using the encounter type table [39].

For in-port cases, where encounter situations frequently change owing to the navigable water area and route configuration, the relative bearing and relative course data of the TSs were extracted based on the first point at which the encounter type remained unchanged until collision.

To accurately classify the characteristics of each collision scenario, in this study, the characteristics were refined into five conditions (Table 4): encounter type, encounter angle, applicable navigation rules, decision-making of the OS, and the number of TSs.

Table 4 Features to be considered for scenarios clustering

Class	Feature	Value	Code
1	Encounter	Overtaking	OT
		Being overtaken	BO
		Head on	HO
		Crossing give-way	CG
		Crossing quarter-lee give-way	QG
		Crossing stand-on	CS
		Crossing quarter-lee stand-on	QS
2	Sector	Sector 1	S1
		Sector 2	S2
		⋮	⋮
		Sector 6	S6
3	Rule	Overtaking	O1
		Overtaking (being overtaken)	O2
		Head on	H
		Crossing (give-way)	C1
		Crossing (stand-on)	C2
4	Action	Give-way (overtaking, head on)	G
		Stand-on (being overtaken)	S
		Multi and complex	M
5	TSs	1 ship	TS1
		2 ships	TS2
		3 ships	TS3
		⋮	⋮
		n ships	TSn

The encounter type and angle clearly describe the encounter situations based on the encounter type table [39], replacing the relative bearing and TS course. The applicable navigation rules and decision-making of the OS indicate: 1) the navigation rules that should be applied in each situation, including scenarios involving multi-ship encounters with three or more ships, and 2) the way in which the OS performs collision-avoidance. Additionally, the number of TSs indicates whether the situation involves a one-on-one or multi-ship encounter.

3.4.3 Collision scenarios clustering

To understand the data structure and design efficient testing scenarios, classifying identical or similar situations across collision scenarios, examining redundancies among the scenarios, and deriving representative scenarios for diverse situations is necessary. Therefore, hierarchical clustering, which is effective for visually representing structural relationships within data, was applied [47].

3.4.3.1 Distance measurement

To calculate the distances during clustering, we employed Hamming distance, considering that the extracted characteristic data for each collision scenario were encoded as strings. Hamming distance is advantageous for measuring string similarity and provides clear interpretability, particularly when the data are relatively simple [48, 49]. Hamming distance is a metric used to measure the difference between two strings or bit sequences. This represents the number of positions at which the corresponding characters in two strings of equal length are different. Hamming distance can be calculated as:

$$D_{Hamming}\,(A,B) = \sum_{i=1}^{n} \mid a_i - b_i \mid \tag{14}$$

Hamming distance was selected because it directly counts mismatches between binary vectors, simplifying the scenario comparison. Unlike metrics such as Euclidean distance or cosine similarity, which are more suitable for continuous or high-dimensional data, Hamming distance provides clear interpretability and efficiency when applied to binary-encoded features.

To apply Hamming distance, the characteristics of each collision scenario were assigned binary values based on the criteria listed in Table 4. As shown in Fig. 14, when the OS and two TSs shared the same encounter type, that is, when multiple TSs had the same characteristics, a binary value of 1 was assigned. This ensured that, for the purpose of clustering, such encounter types were treated as single-ship encounters [50].

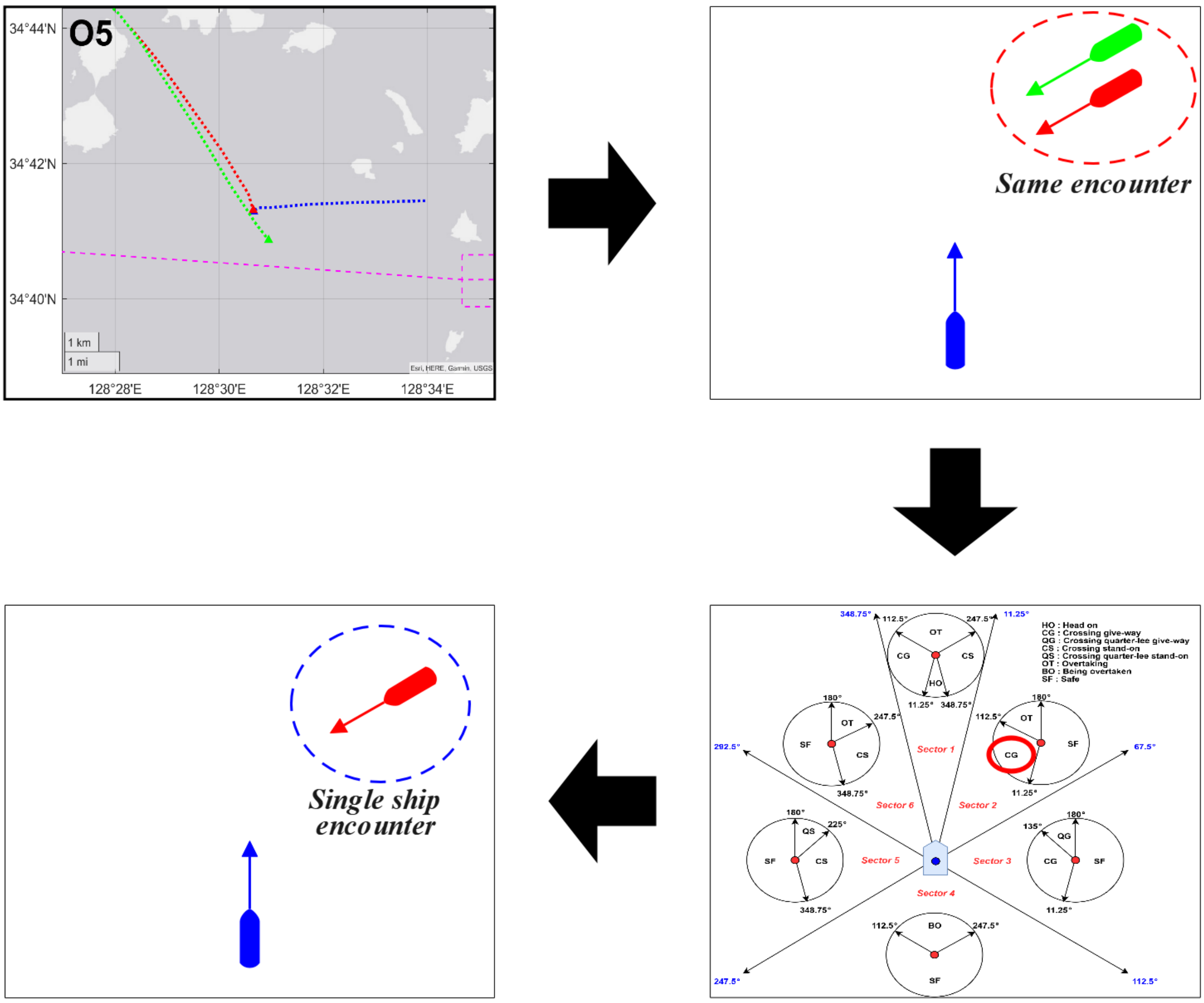

Fig. 14 Combination of ships in the same encounter situation

In the case of collision scenario O5, two TSs were located in Sector 2 with a CG encounter relative to the OS. However, this did not affect the decision-making of the OS as a give-way ship. Therefore, these two TSs were treated as a single ship for encounter type clustering.

An example of calculating Hamming distance between collision scenarios O1 and O1T1 based on the binary vectorised data of situations in the open sea is described in Fig. 15 [48].

Case	Encounter							Sector					
	OT	BO	HO	CG	QG	CS	QS	S1	S2	S3	S4	S5	S6
O1	0	0	0	0	0	1	0	0	0	0	0	0	1
O1T1	0	0	0	1	0	0	0	0	0	1	0	0	0

$$D_{Hamming}(\mathrm{O1},\ \mathrm{O1T1}) = 4$$

Fig. 15 Example of calculating Hamming distance

As the string listing the features of the collision scenarios contained four different values, Hamming distance between collision scenarios O1 and O1T1 was calculated as 4.

3.4.3.2 Linkage method

The linkage method for clustering was determined by comparing the cophenetic correlation coefficient (Fig. 16), which is an evaluation metric for hierarchical clustering [48, 51]. Average linkage method, which demonstrated the best performance, was employed for hierarchical clustering.

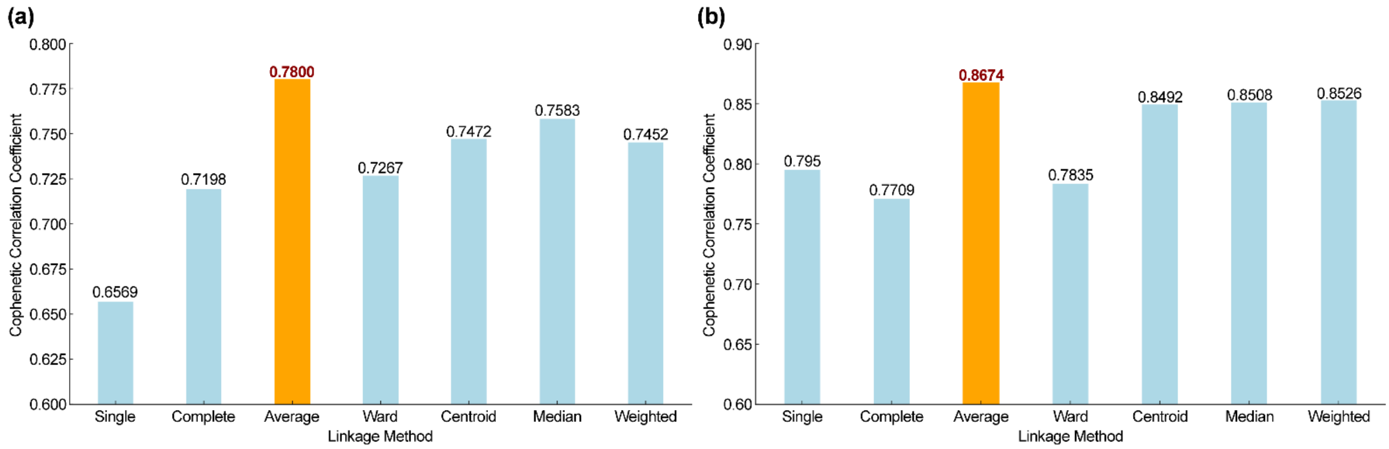

Fig. 16 Cophenetic correlation coefficient for scenarios: (a) open sea, (b) in port

3.4.3.3 Optimal number of clusters

The collision scenarios were classified using hierarchical clustering with Hamming distance, and Average linkage method was applied to the binary vectorised collision data. In this process, determining the optimal number of clusters to group similar data points is necessary while ensuring a clear distinction between the different clusters. Among the various techniques for determining the optimal number of clusters, the mean inter-cluster distance method was used. This method is used to evaluate the degree of separation between clusters and identify the optimal cluster count at the point where the inter-cluster distances are maximised [52].

3.4.3.4 Hierarchical clustering

Hierarchical clustering was conducted to obtain the final clustering result of collision scenarios. The scenarios were merged step by step and visualised in a dendrogram, with a cut-off line used to indicate the resulting cluster structure. This procedure provided a systematic grouping of similar scenarios and established representative sets for subsequent analysis.

3.4.3.5 Algorithm for scenario development

For scenario development, Algorithm 2, mentioned below, was designed. First, the collision scenarios were expanded by altering the OS and TS roles based on the extracted trajectories. Next, the feature values for each collision scenario were extracted. For collision cases in the open sea, features were extracted at the point where the CRI based on FIS-NC [36] reached 0.01. Conversely, for port collision cases, features were extracted at the earliest moment when the encounter type remained unchanged until the collision. Finally, the extracted features were binary vectorised, and hierarchical clustering using Hamming distance was applied to classify the collision scenarios, thereby systematising the collision-avoidance testing scenario set.

Algorithm 2. Scenario development

Input: Set of initial collision scenarios including trajectories of collision ships and influencing ships. [O1(OS, TS1), O2(OS, TS1), O3(OS, TS1, TS2, TS3) …, P7(OS, TS1, TS2)]

Output: Collision-avoidance scenario set [O1, O1T1, O2, O2T1, …, P7, P7T1, P7T2]

% Scenario expansion
FOR each [O1, O2, O3, …, O12, P1, P2, …, P7]
 Change status between OS and TS [TS1, TS2, …, TSn]
  IF collision location = open sea
   Then construct a set of expanded scenarios in open sea [O1, O1T1, O2, …, O12T1]
  IF collision location = in port
   Then construct a set of expanded scenarios in open sea [P1, P1T1, P2, …, P7T2]
Construct collision-avoidance scenario set [O1, O1T1, O2, O2T1, …, P7, P7T1, P7T2]

% Features extraction of each scenario
FOR each [O1, O1T1, O2, O2T1, …, P7, P7T1, P7T2]
 IF collision location = open sea
  THEN extract features in case of min. index of $CRI \geq 0.01$
 IF collision location = in port
  THEN extract features in case of min. index with no encounter change from collision
Construct a set of features [encounter, sector, rule, action, number of TS]

% Scenarios clustering
FOR each [O1, O1T1, O2, O2T1, …, P7, P7T1, P7T2]
 Transform the features into binary vectorised data
  Cluster scenarios using hierarchical clustering with Hamming distance
Construct the final set of collision-avoidance scenarios

---

4. Results and discussion

4.1 Developed scenario sets

Based on the methodology described in Section 3.4.1, additional encounter variations were generated by altering the roles of the OS and TSs. This expansion process yielded 30 supplementary collision scenarios (Fig. 17), comprising 17 in the open sea and 13 in port areas. To ensure systematic identification, the scenario codes were updated by appending the number of the TS whose role was altered (e.g., T1 and T2) to the original scenario code. For example, when the role of TS1 was altered in the open-sea scenario O3, the new code was designated as O3T1. Similarly, altering the role of TS2 in scenario O3 resulted in the code O3T2.

Fig. 17 illustrates the expanded set of collision scenarios, which together with the original cases formed the foundation for a structured scenario dataset employed in subsequent clustering analyses.

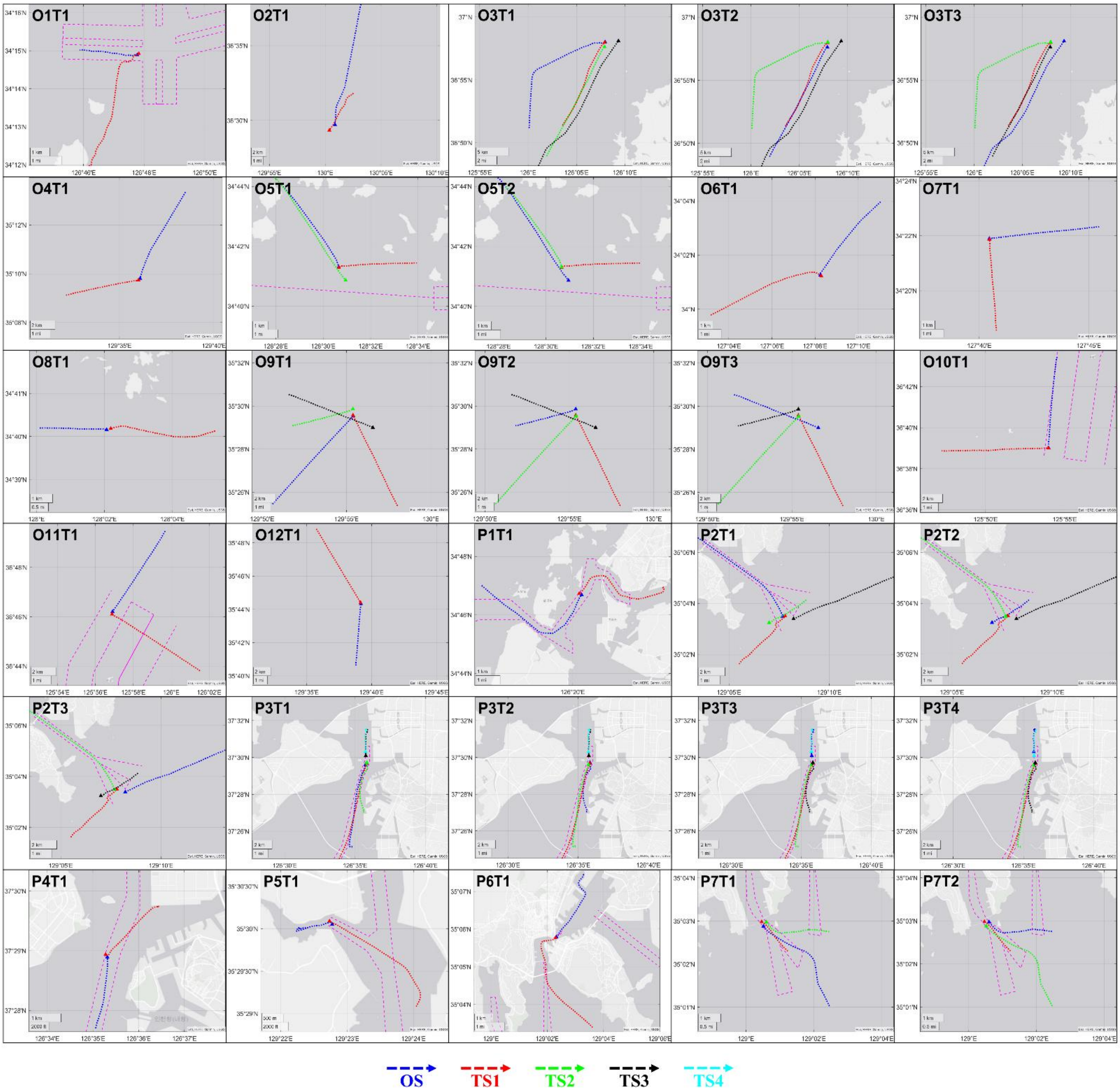

Fig. 17 Expanded collision scenarios

Through this process, the developed testing scenario set, as detailed in Appendix 3, consisted of 49 scenarios: 29 scenarios for the open sea and 20 scenarios for the port. Each scenario included not only the encounter situation and speed at the time but also external factors, such as weather, fairways, and ship information.

4.2 Feature representation

Based on the methodology described in Section 3.4.2, the characteristics of each collision scenario were extracted from the relative bearing and relative course data of the TSs. For the open-sea cases, features were obtained at the point where the FIS-NC-based CRI first reached 0.01, indicating the onset of collision risk (Fig. 18).

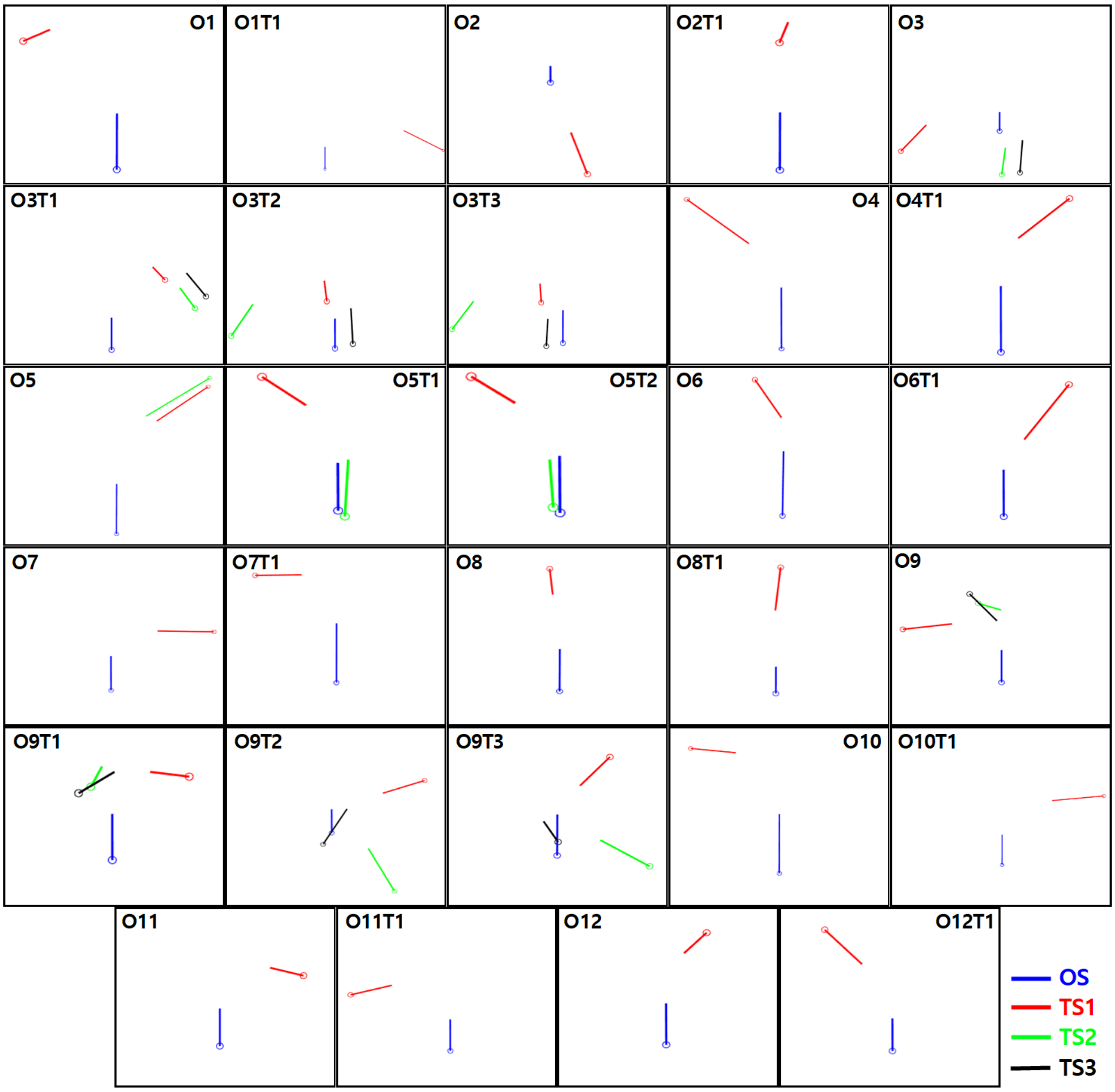

Fig. 18 CRI 0.01 Encounter situations in open sea

The extracted encounter situations were then assigned codes composed of one number and two letters to enable intuitive classification (Table 5). The first number represents the sector of the TS relative to the OS, while the second and third letters indicate the encounter type derived from the encounter type table.

For in-port cases, where encounter situations frequently change owing to restricted waters and route configurations, the features were extracted at the earliest point where the encounter type remained unchanged until the collision (Fig. 19). Similar to the open-sea cases, each in-port scenario was assigned a code based on its sector and encounter type (Table 6).

The extracted features captured not only simple encounters but also complex multi-ship interactions in which the OS acted simultaneously as a give-way ship for one TS and as a stand-on ship for another. These characteristics were then organised into five conditions—encounter type, encounter angle, applicable navigation rules, OS decision-making, and the number of TSs—forming a structured feature set.

The resulting characteristics were visualised as heat maps to illustrate the distribution and frequency of encounter situations. In the open sea (Fig. 20), the OS was most frequently classified as a crossing give-way (CG) or crossing stand-on (CS) vessel, with TSs often located in Sectors 2 and 6. In port encounters (Fig. 21), the OS was again frequently in CG or CS status, but TSs were concentrated in Sector 1, and the OS often held both give-way and stand-on roles simultaneously owing to multi-ship encounters.

Table 5 Encounter type of situations in open sea

Location	Scenario	TS1	TS2	TS3
Open Sea	O1	6CS	-	-
	O1T1	3CG	-	-
	O2	4BO	-	-
	O2T1	1OT	-	-
	O3	5CS	4BO	4BO
	O3T1	2OT	2OT	2OT
	O3T2	1OT	5QS	3QG
	O3T3	6OT	5QS	5QS
	O4	6CS	-	-
	O4T1	2CG	-	-
	O5	2CG	2CG	-
	O5T1	6CS	4BO	-
	O5T2	6CS	6OT	-
	O6	1CS	-	-
	O6T1	2CG	-	-
	O7	2CG	-	-
	O7T1	6CS	-	-
	O8	1HO	-	-
	O8T1	1HO	-	-
	O9	6CS	6CS	6CS
	O9T1	2CG	6OT	6OT
	O9T2	2CG	4BO	4BO
	O9T3	2CG	3CG	1OT
	O10	6CS	-	-
	O10T1	2CG	-	-
	O11	2CG	-	-
	O11T1	6CS	-	-
	O12	2CG	-	-
	O12T1	6CS	-	-

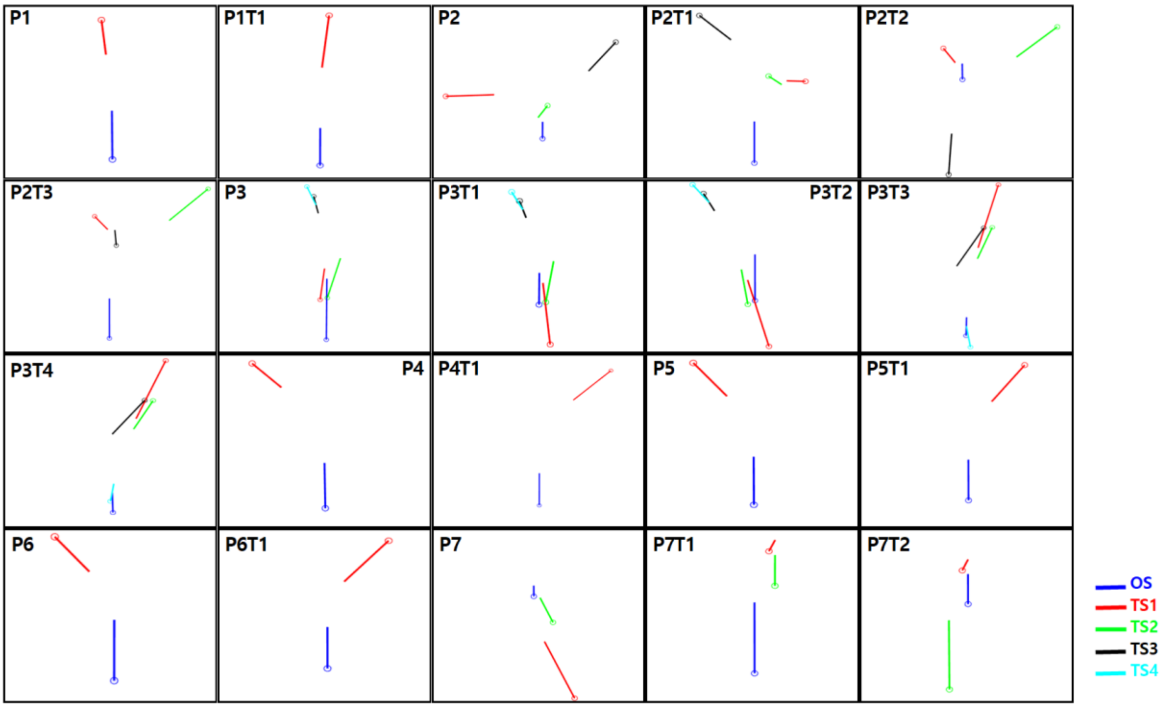

Fig. 19 No change encounter situations in port

Table 6 Encounter type of scenarios in port

Location	Scenario	TS1	TS2	TS3	TS4
In Port	P1	1HO	-	-	-
	P1T1	1HO	-	-	-
	P2	5CS	1CG	1CG	-
	P2T1	2CG	1CS	6CS	-
	P2T2	1CS	2CG	4BO	-
	P2T3	1CS	2CG	2OT	-
	P3	1OT	1OT	1CS	1CS
	P3T1	4BO	2OT	1CS	1CS
	P3T2	4BO	4BO	1CS	6CS
	P3T3	1CG	1CG	1CG	4BO
	P3T4	2CG	2CG	2CG	1OT
	P4	6CS	-	-	-
	P4T1	2CG	-	-	-
	P5	6CS	-	-	-
	P5T1	2CG	-	-	-
	P6	6CS	-	-	-
	P6T1	2CG	-	-	-
	P7	4BO	4BO	-	-
	P7T1	1OT	1OT	-	-
	P7T2	1OT	4BO	-	-

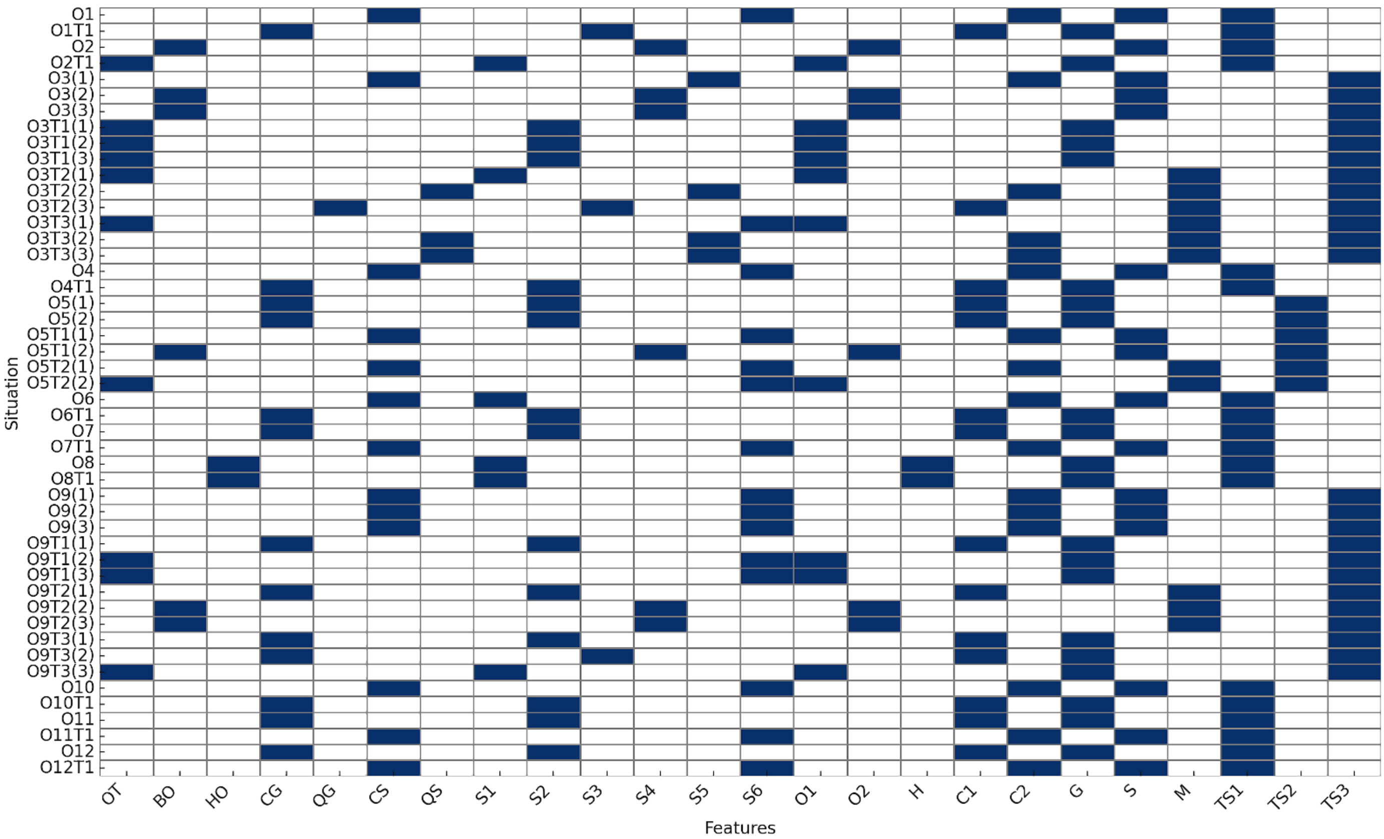

Fig. 20 Heatmap of feature extraction for each scenario in open sea

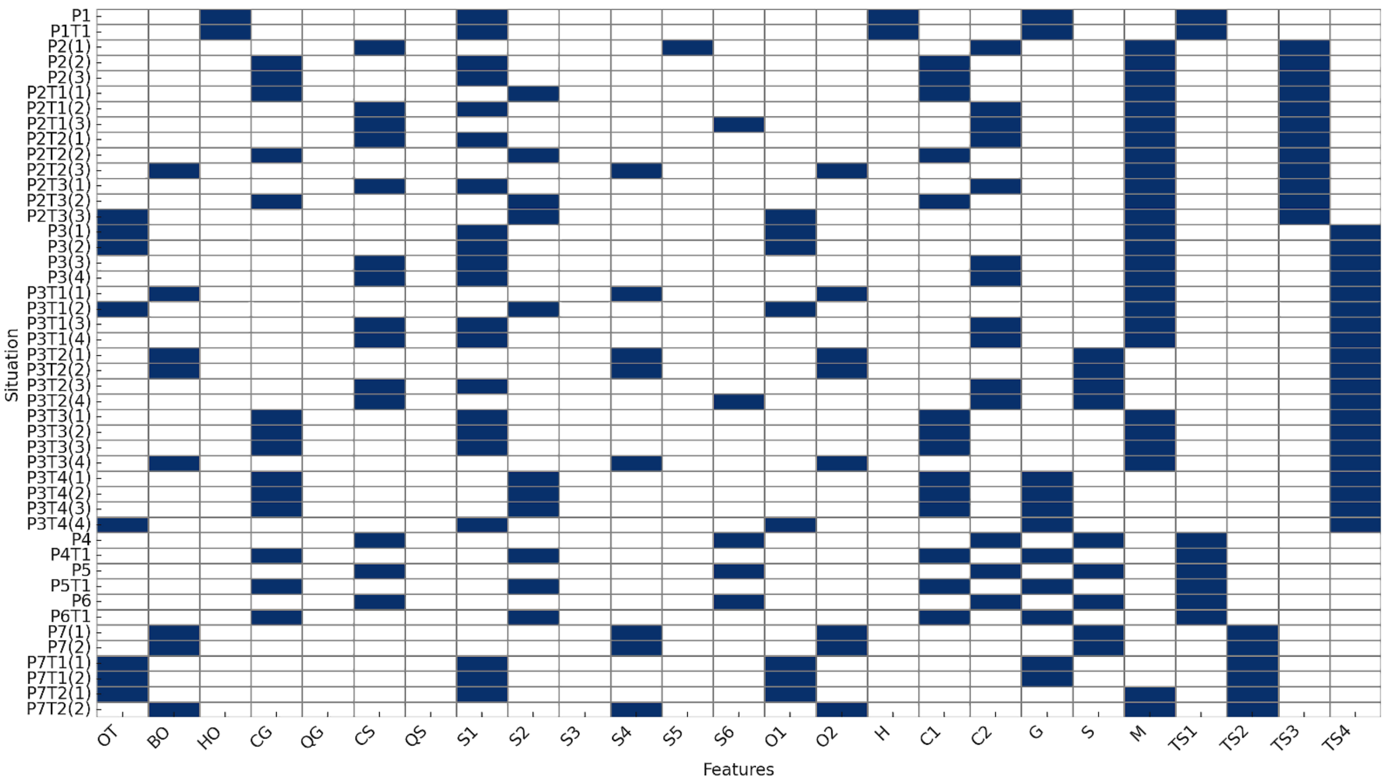

Fig. 21 Heatmap of feature extraction for each scenario in port

The characteristics of the collision scenarios in the open sea and port obtained using this method are summarised in Tables 7 and 8, respectively.

Table 7 Binary vectorised data of scenarios in open sea

Case	Encounter							Sector						Rule					Action			TSs			
	OT	BO	HO	CG	QG	CS	QS	S1	S2	S3	S4	S5	S6	O1	O2	H	C1	C2	G	S	M	TS1	TS2	TS3	TS4
O1	0	0	0	0	0	1	0	0	0	0	0	0	1	0	0	0	0	1	0	1	0	1	0	0	0
O1T1	0	0	0	1	0	0	0	0	0	1	0	0	0	0	0	0	1	0	1	0	0	1	0	0	0
O2	0	1	0	0	0	0	0	0	0	0	1	0	0	0	1	0	0	0	0	1	0	1	0	0	0
O2T1	1	0	0	0	0	0	0	1	0	0	0	0	0	1	0	0	0	0	1	0	0	1	0	0	0
O3	0	1	0	0	0	1	0	0	0	0	1	1	0	0	1	0	0	1	0	1	0	0	0	1	0
O3T1	1	0	0	0	0	0	0	0	1	0	0	0	0	1	0	0	0	0	1	0	0	0	0	1	0
O3T2	1	0	0	0	1	0	1	1	0	1	0	1	0	1	0	0	1	1	0	0	1	0	0	1	0
O3T3	1	0	0	0	0	0	1	0	0	0	0	1	1	1	0	0	0	1	0	0	1	0	0	1	0
O4	0	0	0	0	0	1	0	0	0	0	0	0	1	0	0	0	0	1	0	1	0	1	0	0	0
O4T1	0	0	0	1	0	0	0	0	1	0	0	0	0	0	0	0	1	0	1	0	0	1	0	0	0
O5	0	0	0	1	0	0	0	0	1	0	0	0	0	0	0	0	1	0	1	0	0	0	1	0	0
O5T1	0	1	0	0	0	1	0	0	0	0	1	0	1	0	1	0	0	1	0	1	0	0	1	0	0
O5T2	1	0	0	0	0	1	0	0	0	0	0	0	1	1	0	0	0	1	0	0	1	0	1	0	0
O6	0	0	0	0	0	1	0	1	0	0	0	0	0	0	0	0	0	1	0	1	0	1	0	0	0
O6T1	0	0	0	1	0	0	0	0	1	0	0	0	0	0	0	0	1	0	1	0	0	1	0	0	0
O7	0	0	0	1	0	0	0	0	1	0	0	0	0	0	0	0	1	0	1	0	0	1	0	0	0
O7T1	0	0	0	0	0	1	0	0	0	0	0	0	1	0	0	0	0	1	0	1	0	1	0	0	0
O8	0	0	1	0	0	0	0	1	0	0	0	0	0	0	0	1	0	0	1	0	0	1	0	0	0
O8T1	0	0	1	0	0	0	0	1	0	0	0	0	0	0	0	1	0	0	1	0	0	1	0	0	0
O9	0	0	0	0	0	1	0	0	0	0	0	0	1	0	0	0	0	1	0	1	0	0	0	1	0
O9T1	1	0	0	1	0	0	0	0	1	0	0	0	1	1	0	0	1	0	1	0	0	0	0	1	0
O9T2	0	1	0	1	0	0	0	0	1	0	1	0	0	0	1	0	1	0	0	0	1	0	0	1	0
O9T3	1	0	0	1	0	0	0	1	1	1	0	0	0	1	0	0	1	0	1	0	0	0	0	1	0
O10	0	0	0	0	0	1	0	0	0	0	0	0	1	0	0	0	0	1	0	1	0	1	0	0	0
O10T1	0	0	0	1	0	0	0	0	1	0	0	0	0	0	0	0	1	0	1	0	0	1	0	0	0
O11	0	0	0	1	0	0	0	0	1	0	0	0	0	0	0	0	1	0	1	0	0	1	0	0	0
O11T1	0	0	0	0	0	1	0	0	0	0	0	0	1	0	0	0	0	1	0	1	0	1	0	0	0
O12	0	0	0	1	0	0	0	0	1	0	0	0	0	0	0	0	1	0	1	0	0	1	0	0	0
O12T1	0	0	0	0	0	1	0	0	0	0	0	0	1	0	0	0	0	1	0	1	0	1	0	0	0

Table 8 Binary vectorised data of scenarios in port

Case	Encounter							Sector						Rule					Action			TSs			
	OT	BO	HO	CG	QG	CS	QS	S1	S2	S3	S4	S5	S6	O1	O2	H	C1	C2	G	S	M	TS1	TS2	TS3	TS4
P1	0	0	1	0	0	0	0	1	0	0	0	0	0	0	0	1	0	0	1	0	0	1	0	0	0
P1T1	0	0	1	0	0	0	0	1	0	0	0	0	0	0	0	1	0	0	1	0	0	1	0	0	0
P2	0	0	0	1	0	1	0	1	0	0	0	1	0	0	0	0	1	1	0	0	1	0	0	1	0
P2T1	0	0	0	1	0	1	0	1	1	0	0	0	1	0	0	0	1	1	0	0	1	0	0	1	0
P2T2	0	1	0	1	0	1	0	1	1	0	1	0	0	0	1	0	1	1	0	0	1	0	0	1	0
P2T3	1	0	0	1	0	1	0	1	1	0	0	0	0	1	0	0	1	1	0	0	1	0	0	1	0
P3	1	0	0	0	0	1	0	1	0	0	0	0	0	1	0	0	0	1	0	0	1	0	0	0	1
P3T1	1	1	0	0	0	1	0	1	1	0	1	0	0	1	1	0	0	1	0	0	1	0	0	0	1
P3T2	0	1	0	0	0	1	0	1	0	0	1	0	1	0	1	0	0	1	0	1	0	0	0	0	1
P3T3	0	1	0	1	0	0	0	1	0	0	1	0	0	0	1	0	1	0	0	0	1	0	0	0	1
P3T4	1	0	0	1	0	0	0	1	1	0	0	0	0	1	0	0	1	0	1	0	0	0	0	0	1
P4	0	0	0	0	0	1	0	0	0	0	0	0	1	0	0	0	0	1	0	1	0	1	0	0	0
P4T1	0	0	0	1	0	0	0	0	1	0	0	0	0	0	0	0	1	0	1	0	0	1	0	0	0
P5	0	0	0	0	0	1	0	0	0	0	0	0	1	0	0	0	0	1	0	1	0	1	0	0	0
P5T1	0	0	0	1	0	0	0	0	1	0	0	0	0	0	0	0	1	0	1	0	0	1	0	0	0
P6	0	0	0	0	0	1	0	0	0	0	0	0	1	0	0	0	0	1	0	1	0	1	0	0	0
P6T1	0	0	0	1	0	0	0	0	1	0	0	0	0	0	0	0	1	0	1	0	0	1	0	0	0
P7	0	1	0	0	0	0	0	0	0	0	1	0	0	0	1	0	0	0	0	1	0	0	1	0	0
P7T1	1	0	0	0	0	0	0	1	0	0	0	0	0	1	0	0	0	0	1	0	0	0	1	0	0
P7T2	1	1	0	0	0	0	0	1	0	0	1	0	0	1	1	0	0	0	0	0	1	0	1	0	0

4.3 Clustering results

Fig. 22 presents a graph comparing the mean inter-cluster distances for different numbers of clusters, derived according to the methodology described in Section 3.4.3.

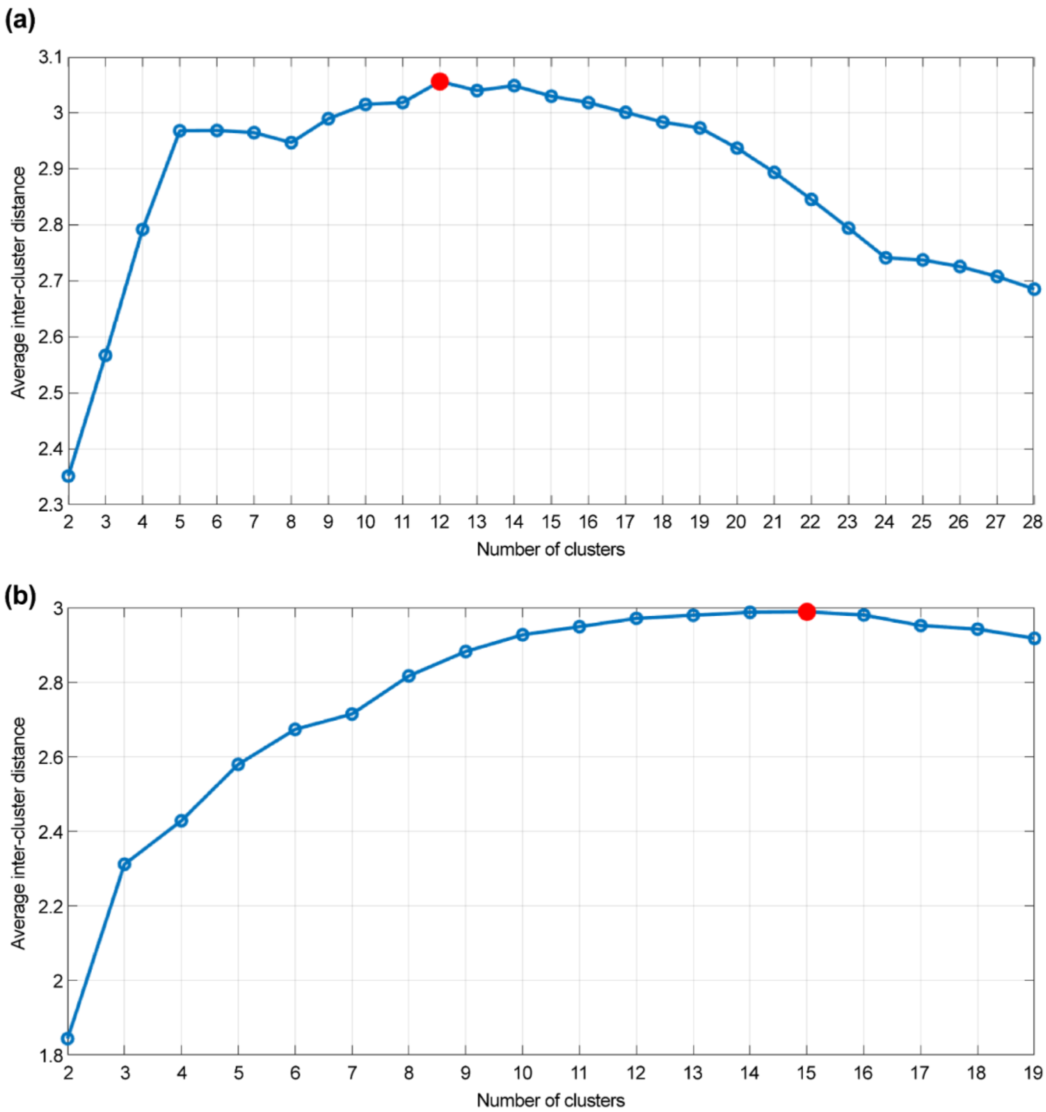

Fig. 22 Average inter-cluster distance for optimal number of clusters: (a) open sea, (b) in port

Fig. 22(a) represents the open-sea scenarios in which the optimal number of clusters was determined to be 12. The optimal number of clusters for the in-port scenarios (Fig. 22(b)) was determined as 15.

Based on the extracted feature data for each collision scenario, hierarchical clustering with Hamming distance and Average linkage method were applied (Fig. 23). The collision scenarios were classified using a dendrogram, where a cut-off line was visualised to intuitively display the optimal number of clusters and the clustering process.

As a result of this clustering, eight collision scenarios, from O11T1 to O6, were grouped into the same cluster for the open-sea cases (Fig. 24(a)), where the ship crossed a stand-on ship. Similarly, the eight collision scenarios from O1T1 to O5 were grouped into another cluster (Fig. 24(b)), where the own-ship was a crossing give-way ship. In addition, O8 and O8T1 were classified as head-on situations (Fig. 24(c)). O3T1 to O9T3 represent multi-ship encounter situations or similar scenarios. The remaining cases were classified as separate encounter situations.

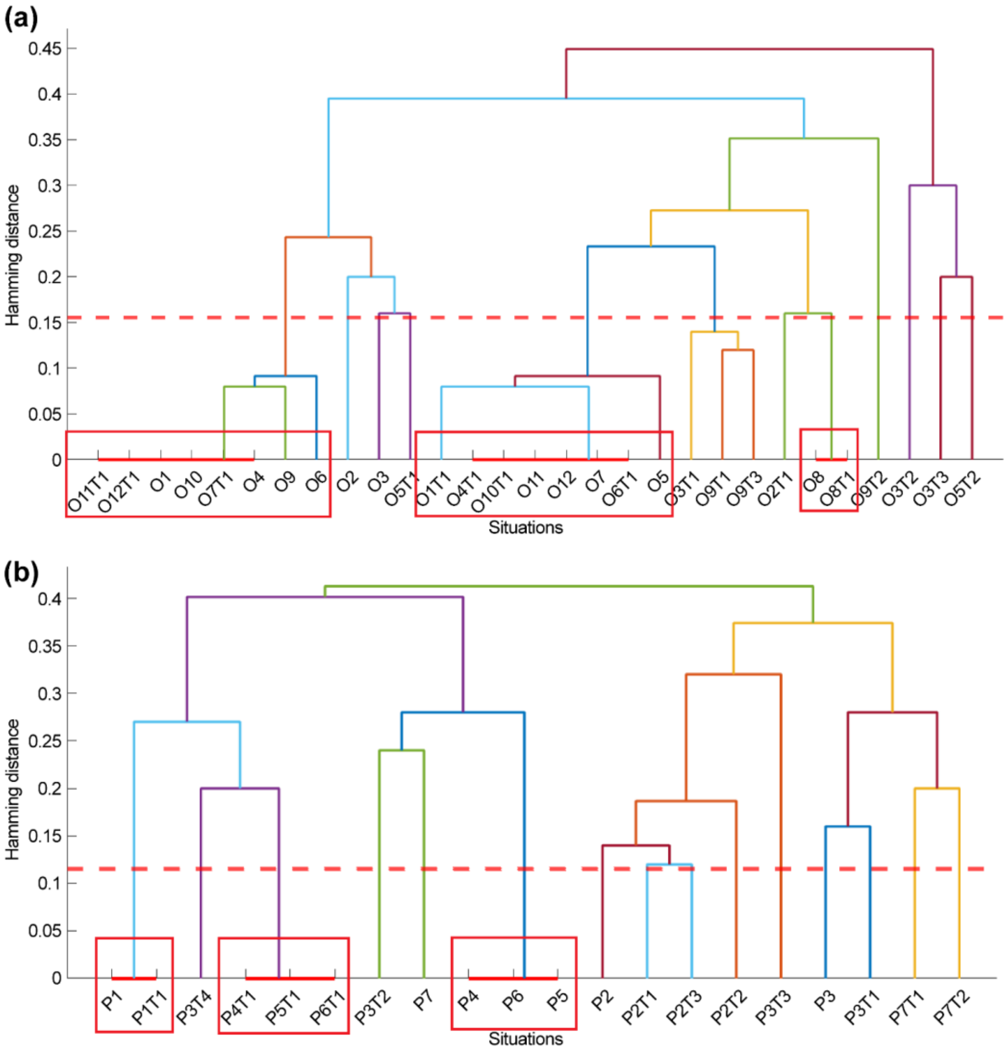

Fig. 23 Dendrogram for collision scenarios: (a) open sea, (b) in port

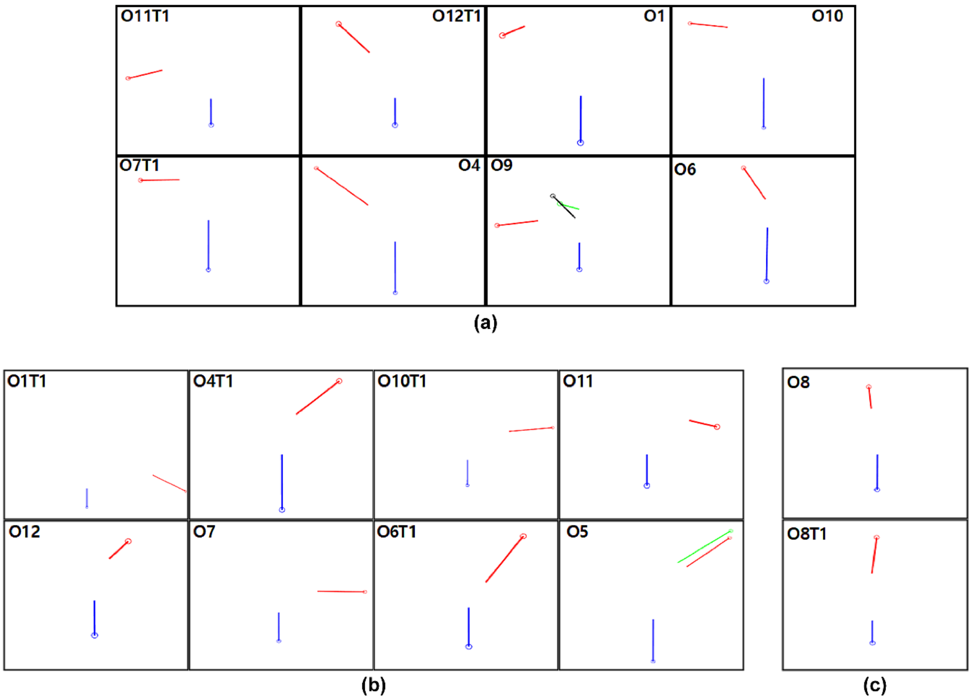

Fig. 24 Cluster of scenarios in open sea

For the in-port cases (Fig. 25), P1 and P1T1 were classified as head-on situations. Collision scenarios P4T1, P5T1, and P6T1 were grouped into the cluster where the OS was the crossing give-way ship, while P4, P5, and P6 were classified into the cluster where the OS was the crossing stand-on ship. The remaining collision scenarios were identified as multi-ship encounters and classified as separate encounters.

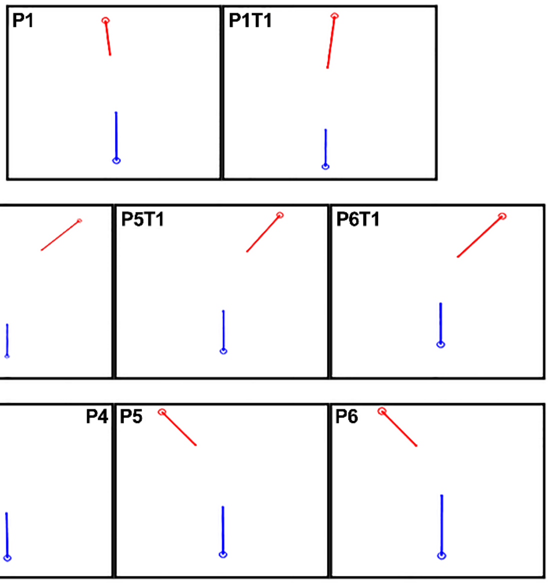

Fig. 25 Cluster of scenarios in port

4.4 Comparison with previous studies: the Imazu problem

The developed scenarios were compared with the Imazu problem [10] (Fig. 26).

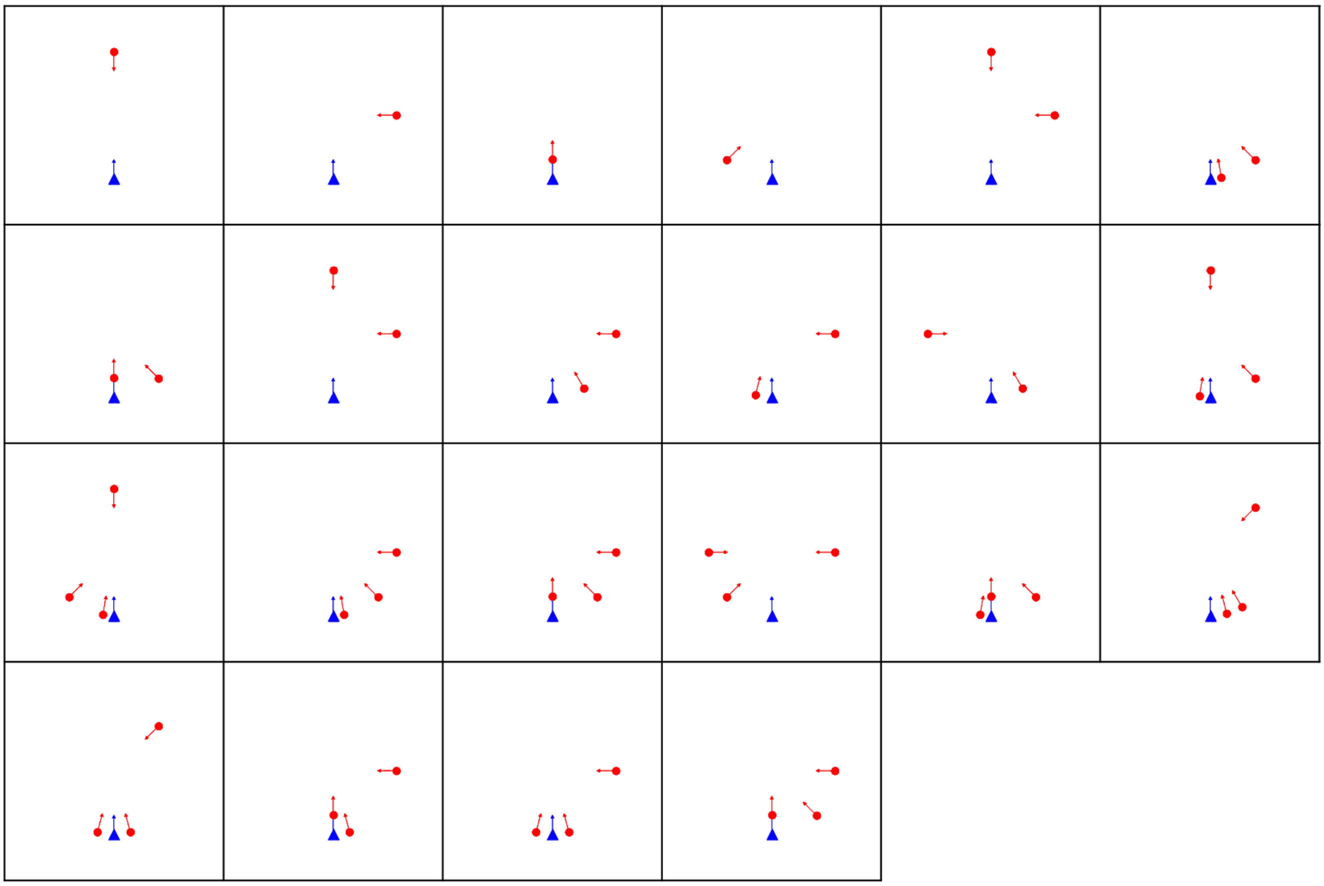

Fig. 26 Basic scenarios of Imazu problem

The initial setting values proposed in the Imazu problem [10, 53] (Table 9) indicate the position ($X_{(\mathrm{nm})}$, $Y_{(\mathrm{nm})}$) and relative course ($\Psi_{(°)}$) of the TS with respect to the OS for each scenario.

Table 9 Setting values of Imazu problem

Cases	TS1			TS2			TS3		
	$X_{(\mathrm{nm})}$	$Y_{(\mathrm{nm})}$	$\Psi_{(°)}$	$X_{(\mathrm{nm})}$	$Y_{(\mathrm{nm})}$	$\Psi_{(°)}$	$X_{(\mathrm{nm})}$	$Y_{(\mathrm{nm})}$	$\Psi_{(°)}$
I1	0	6	180	-	-	-	-	-	-
I2	6	0	−90	-	-	-	-	-	-
I3	0	−4.2	0	-	-	-	-	-	-
I4	−4.243	−4.243	45	-	-	-	-	-	-
I5	0	6	180	6	0	−90	-	-	-
I6	1.042	−5.909	−10	4.243	−4.243	−45	-	-	-
I7	0	−4.2	0	4.243	−4.243	−45	-	-	-
I8	0	6	180	6	0	−90	-	-	-
I9	3	−5.196	−30	6	0	−90	-	-	-
I10	6	0	−90	−1.553	−5.796	15	-	-	-
I11	−6	0	90	3	−5.196	−30	-	-	-
I12	4.243	−4.243	−45	−1.042	−5.909	10	0	6	180
I13	0	6	180	−1.042	−5.909	10	−4.243	−4.243	45
I14	1.042	−5.909	−10	4.243	−4.243	−45	6	0	−90
I15	0	−4.2	0	4.243	−4.243	−45	6	0	−90
I16	−4.243	−4.243	45	−6	0	90	6	0	−90
I17	0	−4.2	0	−1.042	−5.909	10	4.243	−4.243	−45
I18	4.243	4.243	−135	1.553	−5.796	−15	3	−5.196	−30
I19	−1.553	−5.796	15	1.553	−5.796	−15	4.243	4.243	−135
I20	0	−4.2	0	1.553	−5.796	−15	6	0	−90
I21	1.553	−5.796	−15	−1.553	−5.796	15	6	0	−90
I22	0	−4.2	0	4.243	−4.243	−45	6	0	−90

Subsequently, based on the set values, the relative bearing and course of the TS with respect to the OS were calculated. To classify similar collision scenarios, the scenarios were compared with scenarios in the open sea and categorised according to the encounter type table [39]. Each problem was represented by a three-character encounter type code (Table 10).

The Imazu problem assumes encounter situations in the open sea. Therefore, it was compared with the scenarios in the open sea developed in this study. Similar to the process (Section 3) for extracting the features of each collision scenario, the features were extracted based on detailed criteria. Subsequently, the number of collision scenarios corresponding to each feature was visualised and compared between the developed scenarios in the open sea and Imazu problem (Fig. 27).

Table 10 Encounter type of Imazu problem

Cases	TS1	TS2	TS3
I1	1HO	-	-
I2	2CG	-	-
I3	1OT	-	-
I4	5CS	-	-
I5	1HO	2CG	-
I6	3QG	3CG	-
I7	1OT	3CG	-
I8	1HO	2CG	-
I9	3QG	2CG	-
I10	2CG	5QS	-
I11	6CS	3QG	-
I12	3CG	5QS	1HO
I13	1HO	5QS	5CS
I14	3QG	3CG	2CG
I15	1OT	3CG	2CG
I16	5CS	6CS	2CG
I17	1OT	5QS	3CG
I18	2CG	3QG	2OT
I19	5QS	3QG	2CG
I20	1OT	3QG	2CG
I21	3QG	5QS	2CG
I22	1OT	3CG	2CG

An analysis of the graph in Fig. 27 revealed that, in the Imazu problem, the OS was not overtaken, and OS was a stand-on ship relatively rarely. In these scenarios, the TS did not approach from sector 4 and TS approached from sector 6 relatively rarely. This indicates that the Imazu problem was designed based on navigation rules, assuming that the give-way TS adhered to the navigation rules and performed collision-avoidance manoeuvres accordingly.

Hierarchical clustering based on Hamming distance was utilised to compare the encounter situations between scenarios in the open sea and Imazu problem [48, 49]. First, to apply Hamming distance, the features of each collision scenario in the Imazu problem were extracted. For each detailed feature criterion, a value of 1 was assigned if the criterion was met, and 0 otherwise, resulting in the binary vectorisation (Table 11). Subsequently, the binary vectorised features of the collision scenarios were combined with the features of the open-sea scenarios, and hierarchical clustering was performed based on this combined dataset.

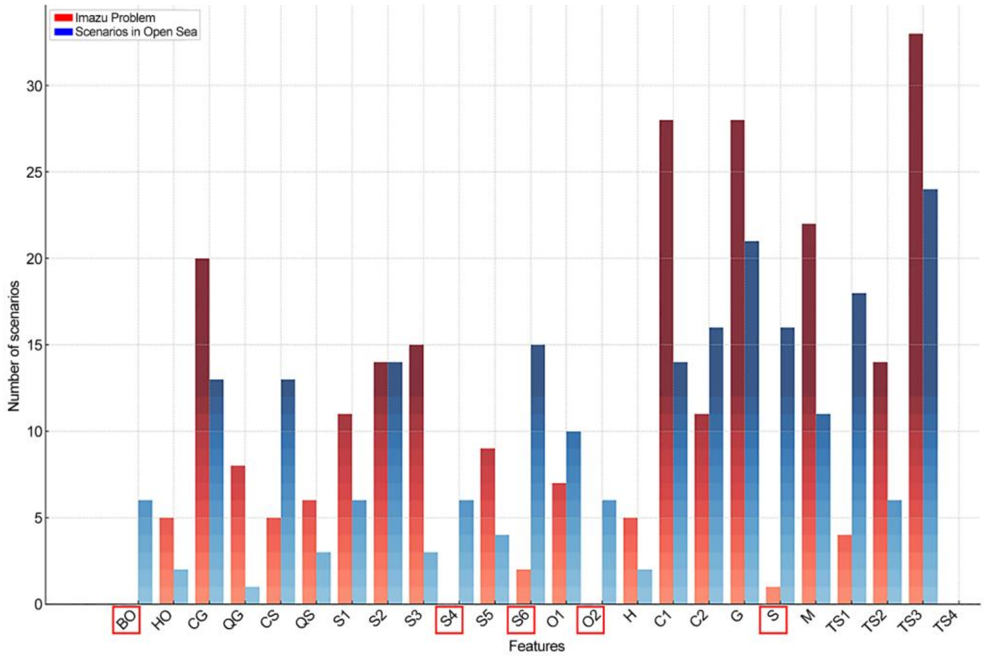

Fig. 27 Number of scenarios of detailed features in open sea + Imazu problem

Table 11 Binary vectorised data of Imazu problem

Cases	Encounter							Sector						Rule					Action			TSs			
	OT	BO	HO	CG	QG	CS	QS	S1	S2	S3	S4	S5	S6	O1	O2	H	C1	C2	G	S	M	TS1	TS2	TS3	TS4
I1	0	0	1	0	0	0	0	1	0	0	0	0	0	0	0	1	0	0	1	0	0	1	0	0	0
I2	0	0	1	0	0	0	0	1	0	0	0	0	0	0	0	1	0	0	1	0	0	1	0	0	0
I3	0	0	0	1	0	1	0	1	0	0	0	1	0	0	0	0	1	1	0	0	1	0	0	1	0
I4	0	0	0	1	0	1	0	1	1	0	0	0	1	0	0	0	1	1	0	0	1	0	0	1	0
I5	0	1	0	1	0	1	0	1	1	0	1	0	0	0	1	0	1	1	0	0	1	0	0	1	0
I6	1	0	0	1	0	1	0	1	1	0	0	0	0	1	0	0	1	1	0	0	1	0	0	1	0
I7	1	0	0	1	0	0	0	1	0	0	0	0	0	1	0	0	1	0	1	0	0	0	0	0	1
I8	1	1	0	0	0	1	0	1	1	0	1	0	0	1	1	0	0	1	0	0	1	0	0	0	1
I9	0	1	0	0	0	1	0	1	0	0	1	0	1	0	1	0	0	1	0	1	0	0	0	0	1
I10	0	1	0	1	0	0	0	1	0	0	1	0	0	0	1	0	1	0	0	0	1	0	0	0	1
I11	1	0	0	1	0	0	0	1	1	0	0	0	0	1	0	0	1	0	1	0	0	0	0	0	1
I12	0	0	0	0	0	1	0	0	0	0	0	0	1	0	0	0	0	1	0	1	0	1	0	0	0
I13	0	0	0	1	0	0	0	0	1	0	0	0	0	0	0	0	1	0	1	0	0	1	0	0	0
I14	0	0	0	0	0	1	0	0	0	0	0	0	1	0	0	0	0	1	0	1	0	1	0	0	0
I15	0	0	0	1	0	0	0	0	1	0	0	0	0	0	0	0	1	0	1	0	0	1	0	0	0
I16	0	0	0	0	0	1	0	0	0	0	0	0	1	0	0	0	0	1	0	1	0	1	0	0	0
I17	0	0	0	1	0	0	0	0	1	0	0	0	0	0	0	0	1	0	1	0	0	1	0	0	0
I18	0	1	0	0	0	0	0	0	0	0	1	0	0	0	1	0	0	0	0	1	0	0	1	0	0
I19	0	0	0	1	0	0	0	0	1	0	0	0	0	0	0	0	1	0	1	0	0	1	0	0	0
I20	0	1	0	0	0	0	0	0	0	0	1	0	0	0	1	0	0	0	0	1	0	0	1	0	0
I21	1	0	0	0	0	0	0	1	0	0	0	0	0	1	0	0	0	0	1	0	0	0	1	0	0
I22	1	1	0	0	0	0	0	1	0	0	1	0	0	1	1	0	0	0	0	0	1	0	1	0	0

In addition, various linkage methods were compared (Fig. 28) using the cophenetic correlation coefficient [51] during hierarchical clustering, and Average linkage method, which demonstrated the best performance, was employed.

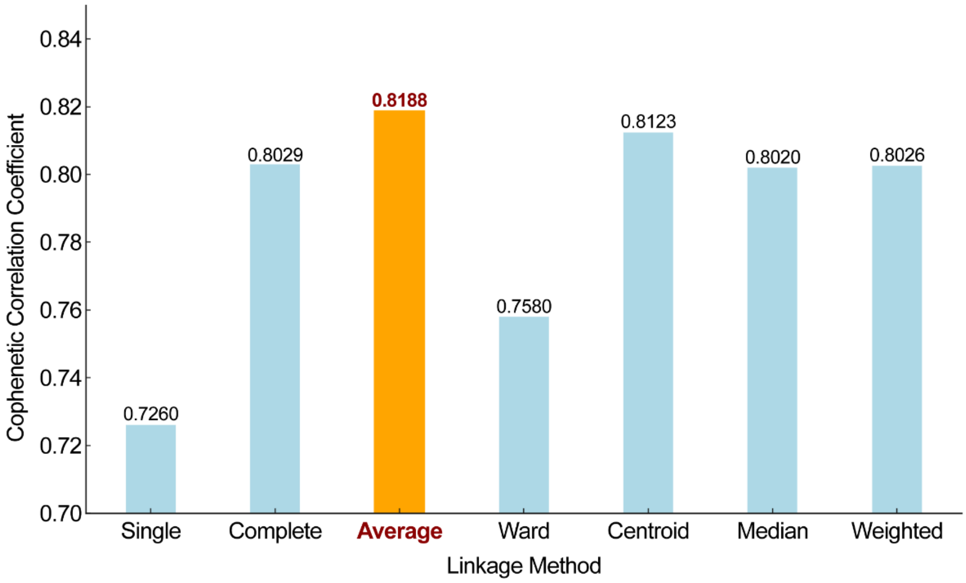

Fig. 28 Cophenetic correlation coefficient for scenarios + Imazu problem

During clustering, the optimal number of clusters was determined using the mean inter-cluster distance method [52]. As shown in Fig. 29, the optimal number of clusters was 22, which corresponded to the cluster count with the largest mean inter-cluster distance.

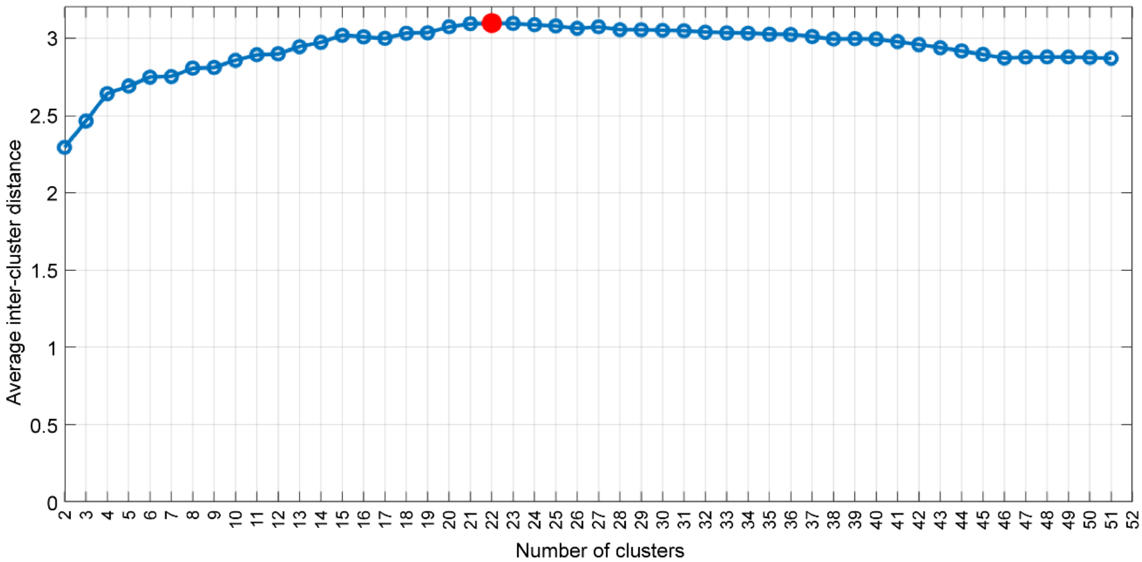

Fig. 29 Average inter-cluster distance for optimal number of clusters

All collision scenarios in the open sea and Imazu problem were classified using a dendrogram based on Hamming distance and Average linkage method (Fig. 30). In addition, the optimal number of clusters was visualised on the dendrogram using a cut-off line determined using the mean inter-cluster distance method.

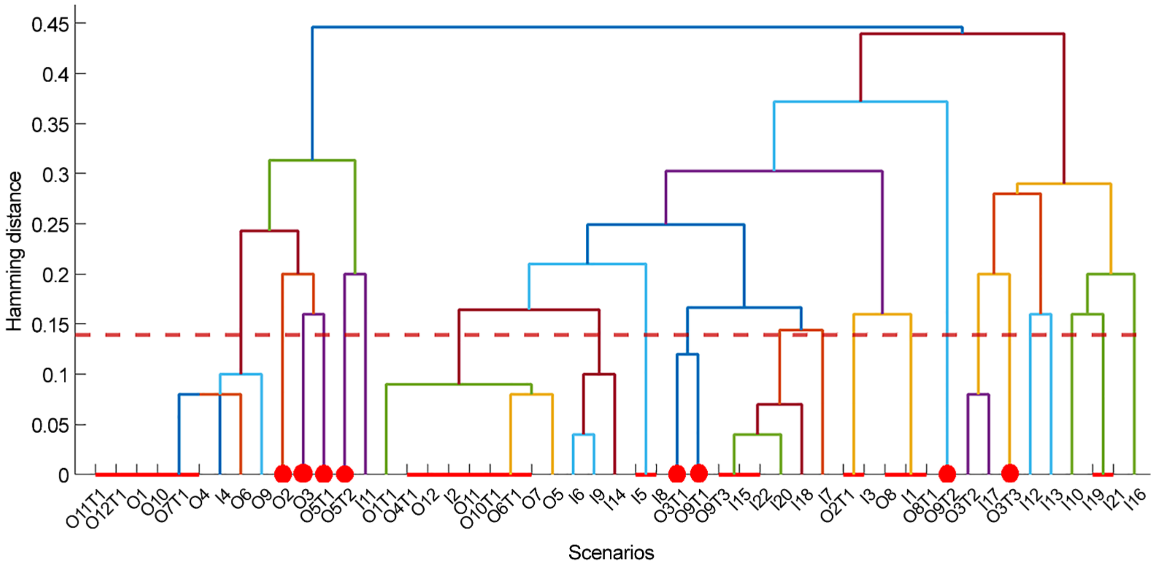

Fig. 30 Dendrogram for scenarios + Imazu problem using Hamming distance

As a result of the clustering, eight scenarios from the developed set were identified as not clustered with the Imazu problem (Fig. 31).

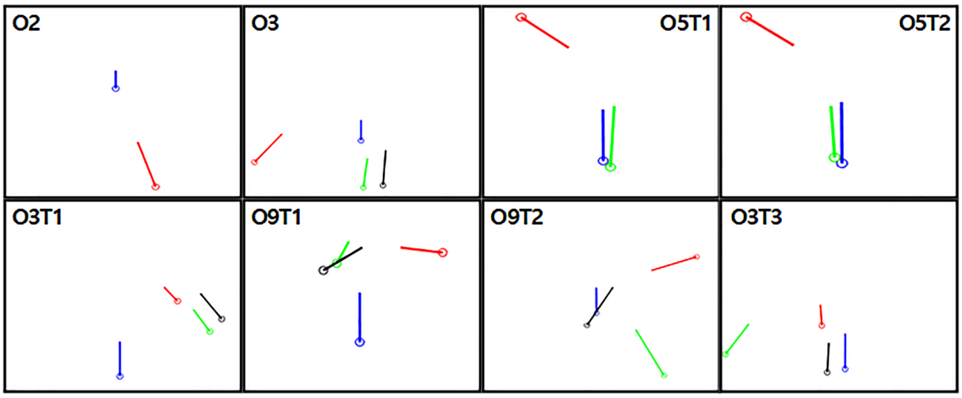

Fig. 31 Scenarios unclustered with Imazu problem

Scenario O2 represents the situation in which OS was overtaken. Scenarios O3 and O5T1 involve multi-ship encounters in which the OS is a stand-on ship in a crossing situation while simultaneously being overtaken. By contrast, scenarios O3T3 and O5T2 represent situations in which the OS is a stand-on ship in a crossing situation while simultaneously overtaking. In addition, scenario O3T1 involves the OS overtaking three TSs, whereas scenarios O9T1 and O9T2 represent multi-ship encounters where the OS is a give-way ship in a crossing situation while simultaneously overtaking or being overtaken. Furthermore, because the scenarios were derived from actual operational trajectories, the encounter types and speeds change continuously, which is a dynamic characteristic particularly evident in port environments (Fig. 32).

The encounter types and speed variations for all scenarios were visualised (Figs. 33 and 34).

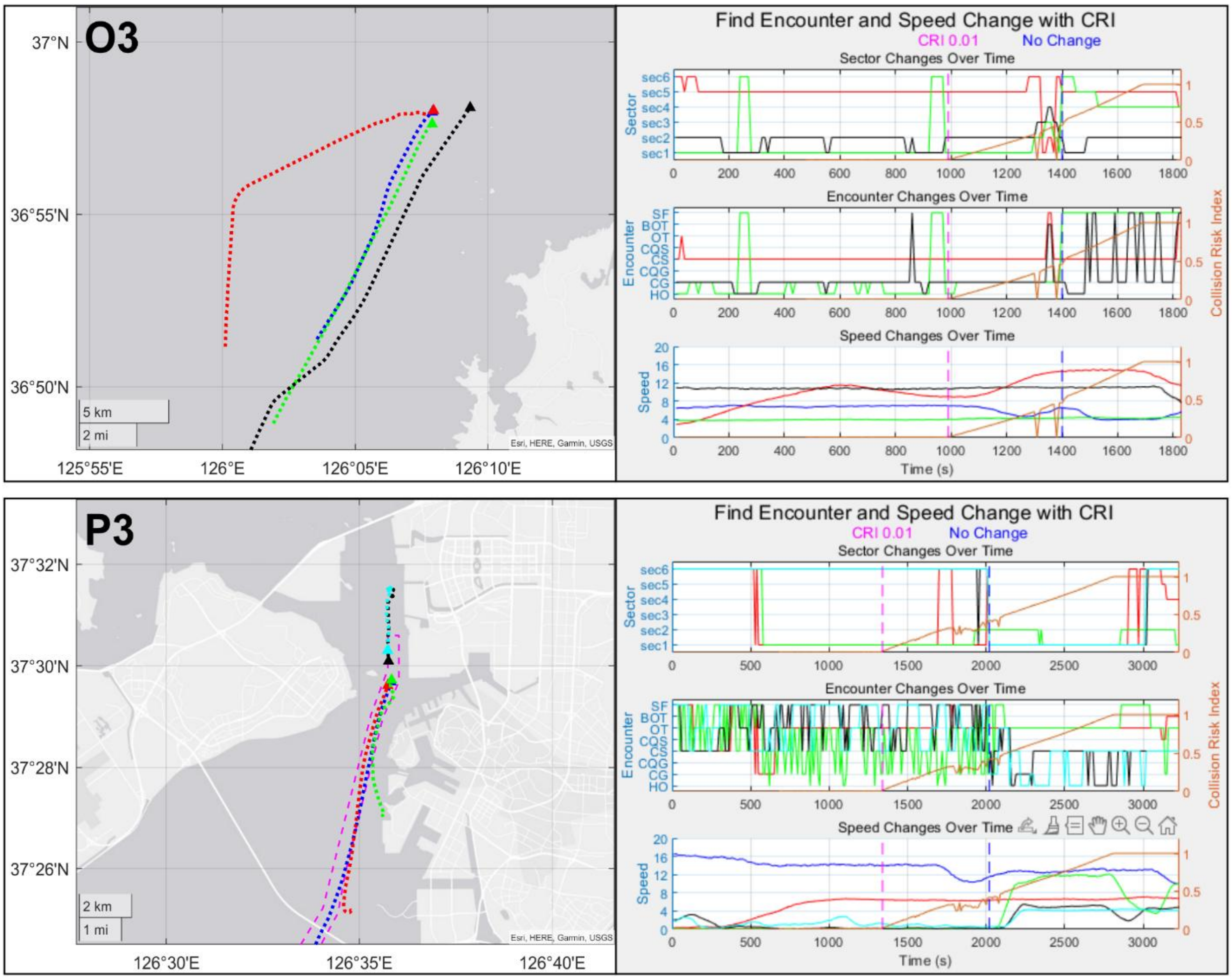

Fig. 32 Changes in encounter and speed for the scenario ‘O3’ and ‘P3’

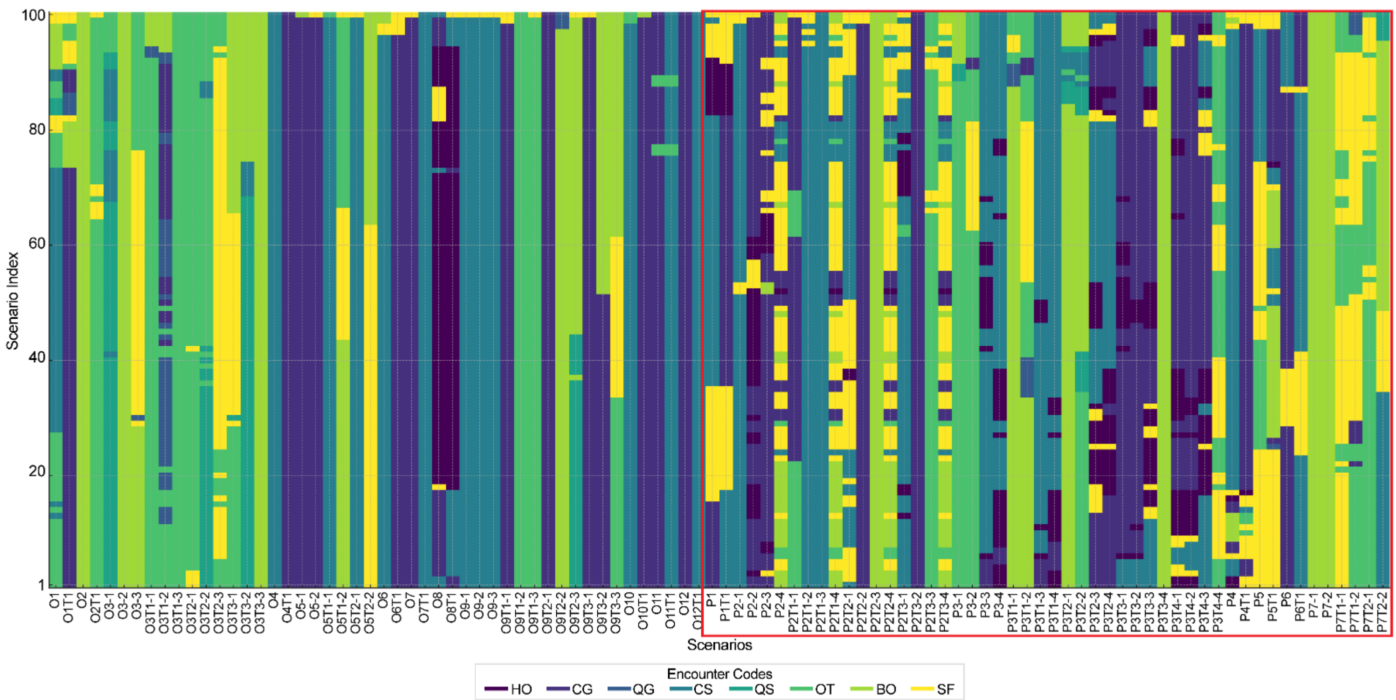

Fig. 33 Heatmap of encounter type changes by scenario

In Fig. 33, the horizontal axis represents the scenario codes, with additional identifiers appended to the multi-ship encounter scenarios to denote specific TSs. The vertical axis indicates the process index for each scenario, where ‘1’ corresponds to the initial encounter situation, and ‘100’ signifies the collision point. The heatmap colours differentiate between encounter types, illustrating their transitions over time. While some scenarios maintained a consistent encounter type from the initial encounter to the collision, the majority exhibited dynamic changes in encounter types as the scenarios progress. These variations are particularly evident on the right side in the heatmap, representing in-port scenarios.

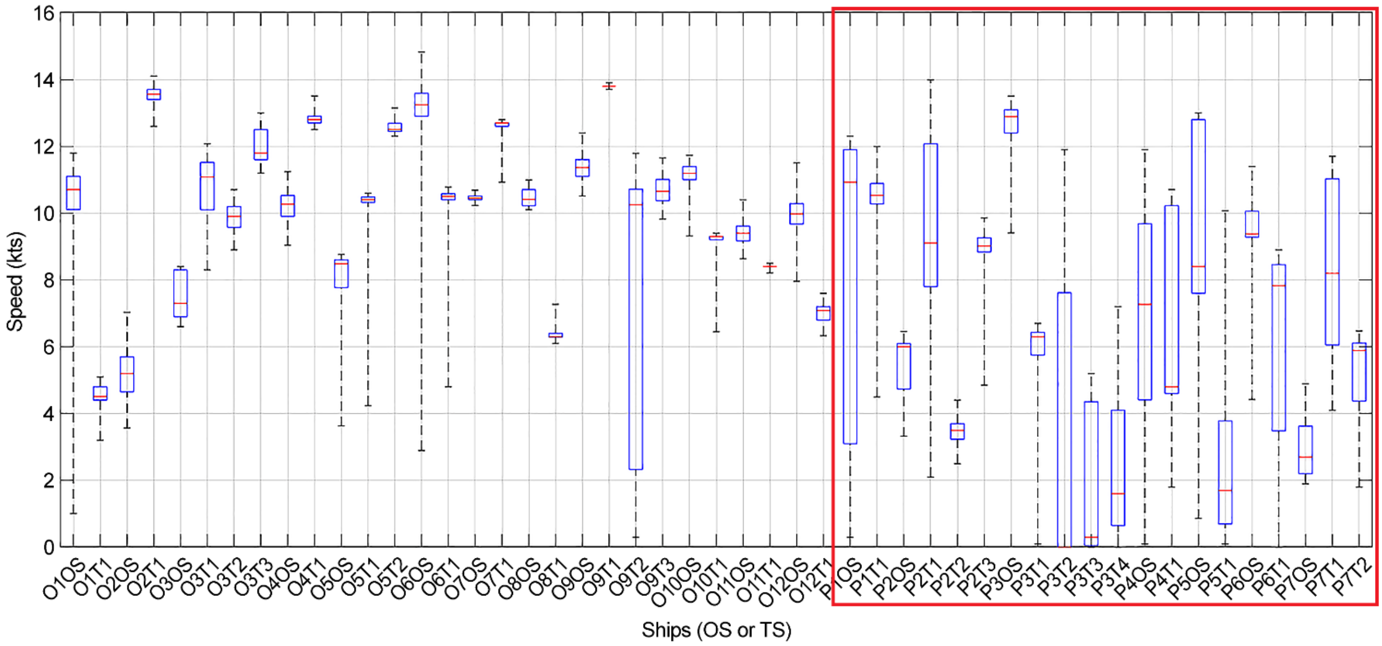

Fig. 34 Boxplot of speed changes by scenario

In Fig. 34, the horizontal axis represents the ship IDs included in each scenario, and the vertical axis indicates the speed of each ship. The speed variations during the progression of each scenario were visualised using boxplots. Although some scenarios exhibited minimal changes in speed, most demonstrated significant speed variations as the scenarios progressed.

As the encounter situation and speed frequently change, the timing of applying navigation rules can significantly influence the decision-making of the OS. Furthermore, continuous monitoring of the situation is required, even after executing a give-way manoeuvre. Particularly, in port scenarios, shown on the right side in each graph, where encounter types and speeds change rapidly and frequently, thoroughly verifying that the collision-avoidance algorithm performs effectively under such dynamic conditions is essential.

4.5 Discussion

In this study, according to the comparison results (Section 4.4), eight scenarios from the developed set were identified as not clustered with the Imazu problem (Fig. 31). Among these, four simple scenarios (O2, O5T2, O3T1, and O3T3), in which the OS is a stand-on ship with no difficulty in cooperative give-way manoeuvres, were excluded. Consequently, a total of four scenarios were identified that were not addressed in the Imazu problem (Fig. 35).

The four newly identified scenarios through the clustering process were multi-ship encounter situations in which various encounter types among ships were intricately intertwined. Additionally, navigation rules were formed between the TSs. This can lead to situations where the OS is put at risk owing to the give-way manoeuvres of the TSs, posing significant challenges to cooperative collision-avoidance manoeuvres. Furthermore, these scenarios hold greater significance because they represent actual collision situations. Therefore, even when the OS is a stand-on ship, situations in which give-way TSs fail to comply with navigation rules or where navigation relationships among TSs in multi-ship encounters affect the OS through their manoeuvres are critical for validating the safety of collision-avoidance algorithms.

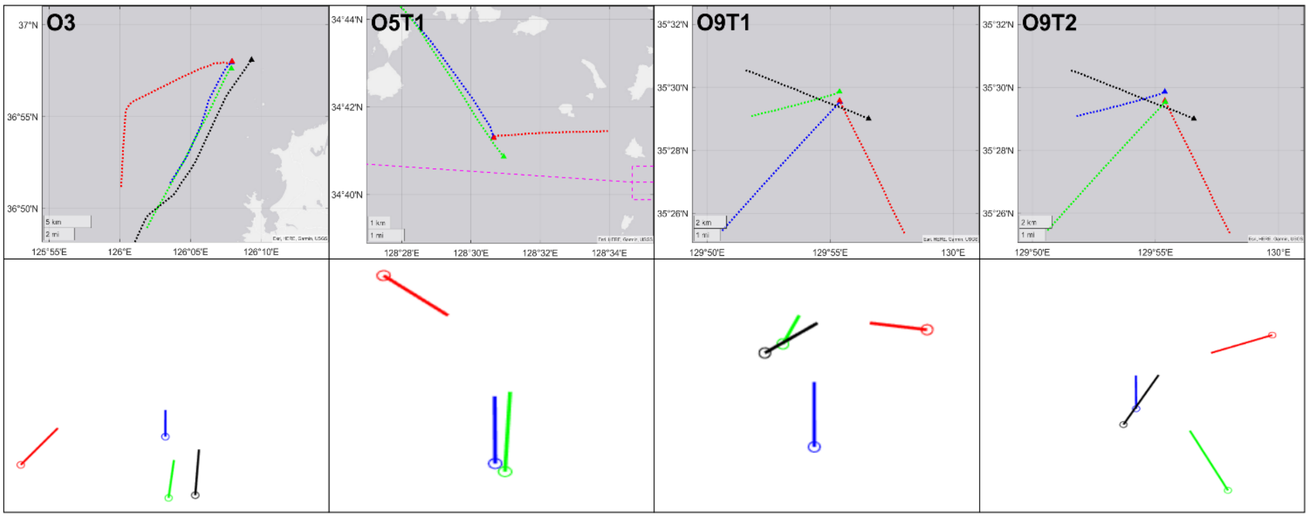

Fig. 35 Final scenarios unclustered with Imazu problem

Additionally, while previous scenarios, including the Imazu problem, address open sea situations, they overlook the characteristics and dynamics of ports. To address this gap, in-port scenarios are considered in this study, offering a more comprehensive scenario framework. In particular, the port scenarios reflect specific conditions absent in open-sea situations, such as navigation rules on fairways, speed restrictions, dynamic courses and speeds, and the presence of arriving and departing ships. While these scenarios may require remote operator intervention, they continue to pose significant challenges for autonomous navigation systems owing to distinct collision risks arising from these conditions.

Furthermore, external environmental factors that could influence collisions, such as weather conditions at the time of the accident, TSS, and ship information, were included. This ensured that even the same encounter situation could unfold into entirely different scenarios, allowing for a multifaceted evaluation of the performance of collision-avoidance algorithms. The advantages of the framework designed in this study compared to previous testing scenarios are summarised in Table 12 [8].

Table 12 Characteristics of testing scenario generation methods

Method	Characteristics contained in the testing scenarios					
	COLREGs non-compliance	**Reality**	**Actual collision**	**Encounter & Speed variation**	**Data in port**	**Environment**
Rule-based	-	-	-	-	-	-
Randomly generated	✓	-	-	-	-	-
Trajectory extraction	✓	✓	-	-	-	-
This study	✓	✓	✓	✓	✓	✓

However, this study considered only actual collision cases from the past five years, which limited its ability to encompass all possible encounter situations at sea. In addition, only domestic collision cases were included, making it essential to expand the scope of scenarios with a broader range of international cases. Furthermore, because only AIS data and information on sailing ships currently in navigation were applied, potential obstacles in the maritime environment, such as fishing ships, anchored ships, and drifting ships, were not considered. Other influential factors, including navigational aids, human and technical elements, and the reliability of investigation reports, were also beyond the scope of this study. Future research should address these limitations.

5. Conclusions

This study developed collision-avoidance testing scenarios based on actual collision accident cases to evaluate the performance of collision-avoidance algorithms for autonomous ships. We designed a framework for developing collision-avoidance testing scenarios based on actual collision cases. The scenarios obtained through the designed framework were subsequently compared with the Imazu problem to identify novel scenarios that were not previously addressed in the Imazu problem. The developed scenarios incorporated actual collision cases and complex situations that cannot be resolved solely by the COLREGs. Additionally, by leveraging detailed accident investigation reports, the developed scenarios accounted for encounter dynamics, speed variations, and external environmental factors such as ship conditions, port operations, prevailing weather, and fairways. These considerations enabled the scenarios to closely mirror actual accident situations and real-world maritime environments, thereby distinguishing them from previous testing scenarios and enhancing the reliability of collision-avoidance algorithm evaluation. Future studies should focus on developing expanded scenarios encompassing all possible sea encounters. This includes integrating diverse data sources, such as existing scenarios based on COLREGs or AIS trajectory data, vessel positioning, alerts, and surveillance systems (V-PASS) [54], e-navigation systems [55], information on fishing ships, anchored or drifting ships, and other maritime obstacles. Leveraging advancements in real-time data collection from comprehensive ship monitoring tools, which capture intricate operational and environmental parameters [56], will be essential for enhancing the realism and applicability of future collision-avoidance scenario generation. Furthermore, incorporating international cases is necessary to expand the scope and applicability of the scenarios. In addition, future research will extend the dataset beyond actual collision accidents to include near-miss situations and ordinary safe encounters. This expansion will turn the proposed framework into a more advanced system for evaluating not only collision-avoidance but also preventive safety (i.e. recognising and responding to potential risks). Finally, applying the scenarios developed in this study to the design and validation of autonomous ship collision-avoidance algorithms remains a crucial task. In particular, the scenarios developed in this study incorporate external environmental factors, and they will be actively utilised for the development and validation of reinforcement-learning-based collision-avoidance algorithms. The proposed framework is not dependent on a specific algorithm and, being based on AIS data, can be applied in a universal manner, thereby serving as a fundamental resource for the future validation of diverse collision-avoidance algorithms for autonomous ships. If such scenarios lead to validated algorithms, they are expected to contribute significantly to reducing maritime accidents and advancing the commercialisation of autonomous ships.

FUNDING

This research was supported by the National University Development Project through the National Research Foundation of Korea, funded by the Ministry of Education.

APPENDIX

Appendix 1 Nomenclature of symbols, abbreviations, and parameters used in this study

Abbreviation /Symbol	Description	Abbreviation /Symbol	Description
AIS	Automatic identification system	L_{ts}	Length of target ship
COLREGs	International regulations for preventing collisions at sea	T_{CPA}	Time to closest point of approach
FIS-NC	Fuzzy inference system based on near-collision	T_s	Standard time
IMO	International maritime organisation	V_{os}	Velocity of own ship
KMST	Korean maritime safety tribunal	V_r	Relative velocity
OS	Own ship	V_{ts}	Velocity of target ship
SD	Ship domain	VCD	Variation of compass degree
TS	Target ship	$V-SD$	Variable ship domain
TSS	Traffic separation scheme	x_{os}, y_{os}	Position of own ship
V-PASS	Vessel positioning, alerts, and surveillance systems	x_{ts}, y_{ts}	Position of target ship
a_{os}	Semi-major axis of own ship	α_r	Relative bearing
a_{ts}	Semi-major axis of target ship	α_{ts}	True bearing of target ship
b_{os}	Semi-minor axis of own ship	θ_{os}	Angle of intersection with respect to a_{os} and x axis
b_{ts}	Semi-minor axis of target ship	θ_{ts}	Angle of intersection with respect to a_{ts} and x axis
CRI	Collision risk index	φ_e	Encounter angle
D_{CPA}	Distance at closest point of approach	φ_r	Relative course
D_r	Relative distance	φ_{os}	Course of own ship
L_{os}	Length of own ship	φ_{ts}	Course of target ship

Appendix 2 Comparison between previous studies

Data Source	Study	Cases	Max. TS	Actual collision	Encounter & Speed variation	Data in port	Environ ment	Subject Ship	Extraction Method
Rule -based	Imazu [10]	42	3	-	-	-	-	-	-
	Wang et al. [12]	54	3	-	-	-	-	-	-
	Sawada et al. [13]	67	2	-	-	-	-	-	Scenario design tool, Time domain
	Chen et al. [14]	5,000	9	-	-	-	-	Length 175/165 m, 8 kn (OS)	Combinatorial-testing-based, Spatiotemporal complexity optimisation
Randomly generated	Porres et al. [16]	∞ * Testing budget: 30,000	1	-	-	-	-	-	Discriminating ANN
	Torben et al. [17]	∞ * Testing budget: 2,911	1	-	-	-	-	Length 8.45 m high-speed	Gaussian process
	Bolbot et al. [18]	∞ * Testing budget: 10,000	2	-	-	-	-	Length 73.7 m, 0–15 kn, 3 nm range	Sobol sequences
Trajectory-extraction	Bakdi et al. [20]	10,000+ (simulation-based)	1 or more	-	-	- (partial use of data)	- (partial use of data)	Realistic ship specs (length/speed varied)	Big maritime traffic data exploitation
	Zhu et al. [5]	2,900	1 or more	-	-	-	-	Encounter lasting for ≥120 s, 6 nm range	Randomly generated on actual encounter
	Hwang and Youn [4]	1,205	1 or more	-	-	-	-	Length 100–130 m, more than 5 kn, 3 nm range	Graph-based modelling, Unit scenarios overlap
	Wang et al. [8]	22,074	1 or more	-	-	-	-	TCPA≤30 min, D_{CPA} 1 nm, 6 nm range	Spatial-temporal proximity
	Dai et al. [21]	∞ * Testing budget: 5	1 or more	-	-	-	✓	Length 225 m, 6 nm range	Virtual-reality integration, Digital twins

[ANN: Artificial neural network]

Appendix 3 Collision-avoidance scenario set

<table>
<tr><th>Scenario</th><th>Encounter (CRI 0.01)</th><th>Speed(kn) (CRI 0.01)</th><th>Scenario</th><th>Wind (dir./ms)</th><th>Current (dir./kn)</th><th>Wave (m)</th><th>Day/Night</th><th>Weather /Visibility</th><th>OS (Length/m)</th><th>TS1 (Length/m)</th><th>Fairway (TSS)</th><th>Others</th></tr>
<tr><td>O1</td><td>6CS</td><td>4.4</td><td rowspan="2">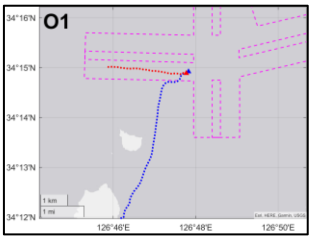
</td><td rowspan="2">SE/6–9</td><td rowspan="2">281°/0.7</td><td rowspan="2">1.0–1.5</td><td rowspan="2">Night</td><td rowspan="2">Cloudy /5 nm</td><td rowspan="2">Passenger/40</td><td rowspan="2">Towing/25</td><td rowspan="2">✓</td><td rowspan="2">-</td></tr>
<tr><td>O1T1</td><td>3CG</td><td>9.3</td></tr>
<tr><td>O2</td><td>4BO</td><td>5.1</td><td rowspan="2">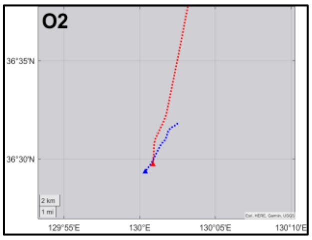
</td><td rowspan="2">SW/5–8</td><td rowspan="2">0</td><td rowspan="2">0.5</td><td rowspan="2">Day</td><td rowspan="2">Cloudy /3 nm</td><td rowspan="2">Towing/11</td><td rowspan="2">General/90</td><td rowspan="2">-</td><td rowspan="2">-</td></tr>
<tr><td>O2T1</td><td>1OT</td><td>13.9</td></tr>
</table>

Scenario	Encounter (*CRI* 0.01)	Speed(kn) (*CRI* 0.01)	Scenario	Wind (dir./ms)	Current (dir./kn)	Wave (m)	Day/Night	Weather /Visibility	OS (Length/m)	TS1 (Length/m)	Fairway (TSS)	Others
O3	5CS/4BO /4BO	11.5/10.2 /12.0	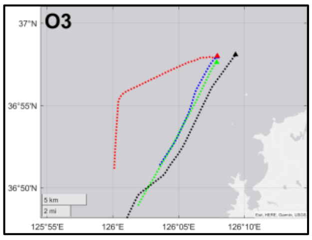	NW/5–7	052°/1.1	1.0	Night	Cloudy /2 nm	Bulk/287	Bulk/80	-	-
O3T1	2OT/2OT /2OT	6.9/10.2 /12.0										
O3T2	1OT/5QS /3QG	7.0/11.4 /11.8										
O3T3	6OT/5QS /5QS	9.2/8.3 /9.8										
O4	6CS	12.9	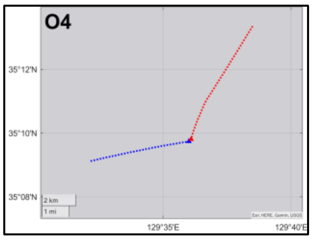	NW/8–9	118°/0.3	2.0	Night	Clear /6 nm	Other/29.33	Tanker/176.20	-	-
O4T1	2CG	9.4										
O5	2CG/2CG	10.3/12.5	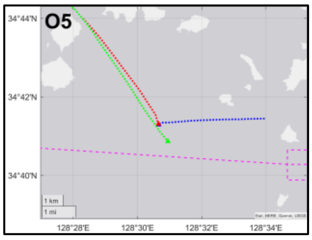	NW/4–6	264°/0.2	0.5	Day	Clear /5 nm	Tanker/35.05	Other/27.24	-	-
O5T1	6CS/4BO	8.5/12.5										
O5T2	6CS/6OT	8.7/10.4										
O6	1CS	10.5	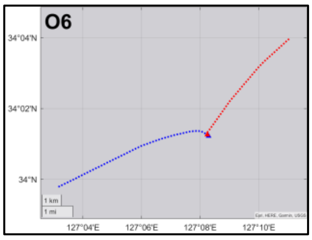	NW /10–12	296°/0.2	1.0–1.5	Night	Clear /7 nm	Other/41.28	CNTR/119.4	-	-
O6T1	2CG	13.5										
O7	2CG	12.7	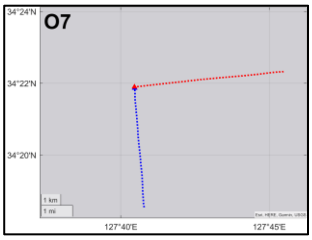	NW/6–8	321°/0.3	0.5–1.0	Night	Clear /7 nm	Other/39.91	General/94.79	-	-
O7T1	6CS	10.3										
O8	1HO	6.3	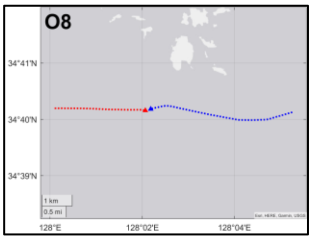	NE/4–5	264°/0.7	0.5	Night	Clear /3 nm	Tanker/39.38	Tanker/49.30	-	-
O8T1	1HO	10.2										

<table>
<tr><th>Scenario</th><th>Encounter
(CRI 0.01)</th><th>Speed(kn)
(CRI 0.01)</th><th>Scenario</th><th>Wind
(dir./ms)</th><th>Current
(dir./kn)</th><th>Wave
(m)</th><th>Day/Night</th><th>Weather
/Visibility</th><th>OS
(Length/m)</th><th>TS1
(Length/m)</th><th>Fairway
(TSS)</th><th>Others</th></tr>
<tr><td>O9</td><td>6CS/6CS
/6CS</td><td>13.8/10.8
/10.7</td><td rowspan="4">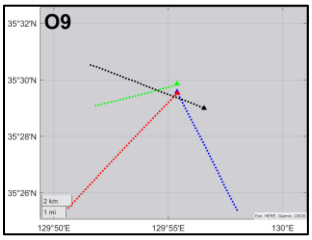</td><td rowspan="4">NE/8–10</td><td rowspan="4">032°/0.2</td><td rowspan="4">1.5</td><td rowspan="4">Night</td><td rowspan="4">Clear
/5 nm</td><td rowspan="4">Other/23.61</td><td rowspan="4">Tanker/146</td><td rowspan="4">-</td><td rowspan="4">-</td></tr>
<tr><td>O9T1</td><td>2CG/6OT
/6OT</td><td>11.2/10.7
/10.7</td></tr>
<tr><td>O9T2</td><td>2CG/4BO
/4BO</td><td>13.7/11.1
/10.7</td></tr>
<tr><td>O9T3</td><td>2CG/3CG
/1OT</td><td>11.3/13.8
/10.0</td></tr>
<tr><td>O10</td><td>6CS</td><td>9.2</td><td rowspan="2">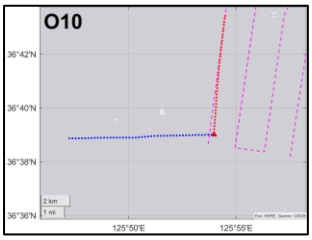</td><td rowspan="2">S/2–4</td><td rowspan="2">030°/0.7</td><td rowspan="2">0.5</td><td rowspan="2">Day</td><td rowspan="2">Clear
/3 nm</td><td rowspan="2">Tanker/86.90</td><td rowspan="2">Other/30.83</td><td rowspan="2">✓</td><td rowspan="2">-</td></tr>
<tr><td>O10T1</td><td>2CG</td><td>11.6</td></tr>
<tr><td>O11</td><td>2CG</td><td>8.4</td><td rowspan="2">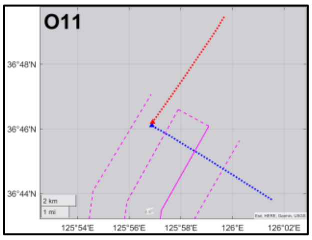</td><td rowspan="2">NW/2–4</td><td rowspan="2">034°/1.9</td><td rowspan="2">0.5</td><td rowspan="2">Night</td><td rowspan="2">Clear
/5 nm</td><td rowspan="2">Other/22.88</td><td rowspan="2">General/113.14</td><td rowspan="2">✓</td><td rowspan="2">-</td></tr>
<tr><td>O11T1</td><td>6CS</td><td>10.0</td></tr>
<tr><td>O12</td><td>2CG</td><td>7.2</td><td rowspan="2">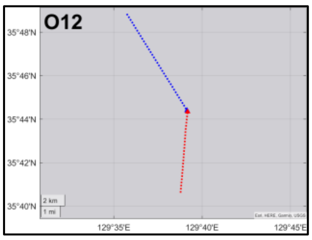</td><td rowspan="2">NW
/10–12</td><td rowspan="2">204°/0.2</td><td rowspan="2">2.0–3.0</td><td rowspan="2">Night</td><td rowspan="2">Cloudy
/1 nm</td><td rowspan="2">Other/21.93</td><td rowspan="2">General/75.03</td><td rowspan="2">-</td><td rowspan="2">-</td></tr>
<tr><td>O12T1</td><td>6CS</td><td>9.9</td></tr>
</table>

Scenario	Encounter (No change)	Speed(kn) (No change)	Scenario	Wind (dir./ms)	Current (dir./kn)	Wave (m)	Day/Night	Weather /Visibility	OS (Length/m)	TS1 (Length/m)	Fairway (TSS)	Others
P1	1HO	10.4	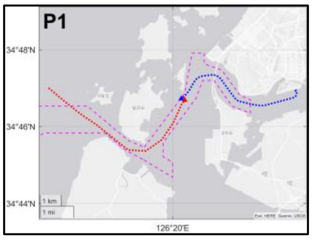	NE/6–8	263˚/0.3	1.0	Night	Cloudy /2 nm	RORO/140	Other/36	✓	Speed limit: 12 kn
P1T1	1HO	11.8										
P2	5CS/1CG /1CG	13.4/4.0 /9.1	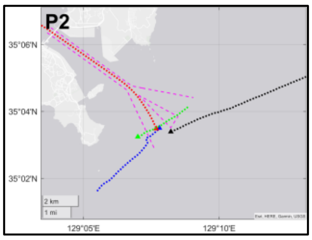	NW/3–4	218˚/0.6	0.5	Day	Clear /3 nm	Towing/30.6	Cruise/347.7	✓	Speed limit: 10 kn
P2T1	2CG/1CS /6CS	4.1/4.0 /9.2										
P2T2	1CS/2CG 4BO	6.3/7.9 /9.1										
P2T3	1CS/2CG 2OT	4.1/13.6 /4.2										
P3	1OT/1OT /1CS/1CS	6.5/11.7 /4.7/4.1	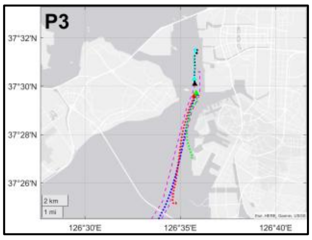	NW/2–4	355˚/4.5	0.5	Night	Clear /3 nm	Tanker/112.37	Towing/42.50	✓	Speed limit: 8 kn
P3T1	4BO/2OT 1CS/1CS	12.2/11.7 /4.7/4.1										
P3T2	4BO/4BO /1CS/6CS	12.1/6.4 /4.5/4.1										
P3T3	1CG/1CG /1CG/4BO	6.6/12.6 /4.3/4.2										
P3T4	2CG/2CG /2CG/1OT	6.7/12.8 /3.9/4.6										
P4	6CS	4.6	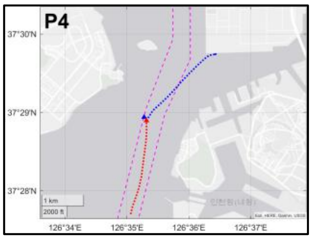	SW/4–6	032˚/1.3	0.5	Night	Clear /3 nm	General/79.31	Towing/33.07	✓	Speed limit: 8 kn
P4T1	2CG	7.3										
P5	6CS	8.3	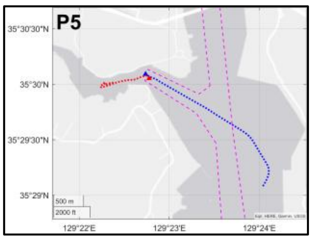	NE/4–8	0	0.5	Day	Clear /7 nm	Tanker/79.99	Tanker/69.72	✓	-
P5T1	2CG	7.9										

<table>
<tr><th>Scenario</th><th>Encounter (No change)</th><th>Speed(kn) (No change)</th><th>Scenario</th><th>Wind (dir./ms)</th><th>Current (dir./kn)</th><th>Wave (m)</th><th>Day/Night</th><th>Weather /Visibility</th><th>OS (Length/m)</th><th>TS1 (Length/m)</th><th>Fairway (TSS)</th><th>Others</th></tr>
<tr><td>P6</td><td>6CS</td><td>8.9</td><td rowspan="2">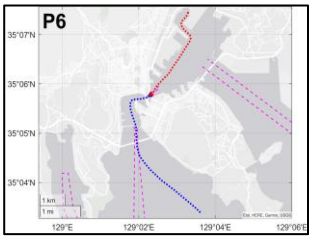
</td><td rowspan="2">SW/6–8</td><td rowspan="2">044°/0.5</td><td rowspan="2">0.5</td><td rowspan="2">Night</td><td rowspan="2">Clear /3 nm</td><td rowspan="2">Tanker/29.38</td><td rowspan="2">Tanker/33.02</td><td rowspan="2">✓</td><td rowspan="2">Speed limit: 8 kn</td></tr>
<tr><td>P6T1</td><td>2CG</td><td>11.2</td></tr>
<tr><td>P7</td><td>4BO/4BO</td><td>10.5/5.9</td><td rowspan="3">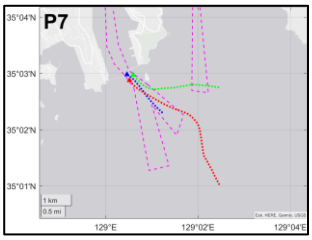
</td><td rowspan="3">SW/2–3</td><td rowspan="3">345°/0.1</td><td rowspan="3">0.5</td><td rowspan="3">Day</td><td rowspan="3">Clear /3 nm</td><td rowspan="3">Towing/Barge 29.06(103.77)</td><td rowspan="3">General/97.77</td><td rowspan="3">✓</td><td rowspan="3">Speed limit: 10 kn</td></tr>
<tr><td>P7T1</td><td>1OT/1OT</td><td>4.0/5.9</td></tr>
<tr><td>P7T2</td><td>1OT/4BO</td><td>6.4/4.6</td></tr>
</table>

REFERENCES

[1] Rødseth, Ø.J., Burmeister, H.C., 2015. Risk assessment for an unmanned merchant ship. *International Journal on Marine Navigation and Safety of Sea Transportation*, 9, 357–364. https://doi.org/10.12716/1001.09.03.08

[2] IMO, 2024. 1972 (COLREGs). Convention on the international regulations for preventing Collisions at sea. https://www.imo.org/en/About/Conventions/Pages/COLREG.aspx (accessed 23rd September 2025).

[3] Zaccone, R., 2021. COLREG-compliant optimal path planning for real-time guidance and control of autonomous ships. *Journal of Marine Science and Engineering*, 9(4), 405. https://doi.org/10.3390/jmse9040405

[4] Hwang, T., Youn, I.-H., 2023. Development of a graph-based collision risk situation model for validation of autonomous ships' collision avoidance systems. *Journal of Marine Science and Engineering*, 11, 2037. https://doi.org/10.3390/jmse11112037

[5] Zhu, F., Zhou, Z., Lu, H., 2022. Randomly testing an autonomous collision avoidance system with real-world ship encounter scenario from AIS data. *Journal of Marine Science and Engineering*, 10, 1588. https://doi.org/10.3390/jmse10111588

[6] Zheng, K., Zhang, X., Wang, C., Li, Y., Cui, J., Jiang, L., 2024. Adaptive collision avoidance decisions in autonomous ship encounter scenarios through rule-guided vision supervised learning. *Ocean Engineering*, 297, 117096. https://doi.org/10.1016/j.oceaneng.2024.117096

[7] Lee, D., Kim, J., 2026. Improving anchorage occupancy forecasting with stacked ensemble learning. *Brodogradnja*, 77(1), 77103. https://doi.org/10.21278/brod77103

[8] Wang, W., Huang, L., Liu, K., Zhou, Y., Yuan, Z., Xin, X., Wu, X., 2024. Ship encounter scenario generation for collision avoidance algorithm testing based on AIS data. *Ocean Engineering*, 291, 116436. https://doi.org/10.1016/j.oceaneng.2023.116436

[9] Hasegawa, K., Fukuto, J., Miyake, R., Yamazaki, M., 2012. An intelligent ship handling simulator with automatic collision avoidance function of target ships. *Proceedings of the 17th International Navigation Simulator Lecturers' Conference (INSLC)*, 3-7 September, Rostock-Warnemuende, Germany.

[10] Imazu, H., 1987. Research on collision avoidance manoeuvre (in Japanese). University of Tokyo, Tokyo, Japan.

[11] Wang, S., Zhang, Y., Zheng, Y., 2021. Multi-ship encounter situation adaptive understanding by individual navigation intention inference. *Ocean Engineering*, 237, 109612. https://doi.org/10.1016/j.oceaneng.2021.109612

[12] Wang, S., Zhang, Y., Zhang, X., Gao, Z., 2023. A novel maritime autonomous navigation decision-making system: modeling, integration, and real ship trial. *Expert Systems With Applications*, 222. https://doi.org/10.1016/j.eswa.2023.119825

[13] Sawada, R., Sato, K., Minami, M., 2024. Framework of safety evaluation and scenarios for automatic collision avoidance algorithm. *Ocean Engineering*, 300, 117506. https://doi.org/10.1016/j.oceaneng.2024.117506

[14] Chen, L., Wang, K., Liu, K., Zhou, Y., Hao, G., Wang, Y., Li, S., 2025. Combinatorial-testing-based multi-ship encounter scenario generation for collision avoidance algorithm evaluation. *Journal of Marine Science and Engineering*, 13, 338. https://doi.org/10.3390/jmse13020338

[15] Ståhlberg, K., Goerlandt, F., Ehlers, S., Kujala, P., 2013. Impact scenario models for probabilistic risk-based design for ship–ship collision. *Marine Structures*, 33, 238-264. https://doi.org/10.1016/j.marstruc.2013.06.006

[16] Porres, I., Azimi, S., Lilius, J., 2020. Scenario-based testing of a ship collision avoidance system. *46th Euromicro Conference on Software Engineering and Advanced Applications (SEAA)*. 26-28 August, Portorož, Slovenija. https://doi.org/10.1109/SEAA51224.2020.00090

[17] Torben, T.R., Glomsrud, J.A., Pedersen, T.A., Utne, I.B., Sørensen, A.J., 2023. Automatic simulation-based testing of autonomous ships using Gaussian processes and temporal logic. *Proceedings of the Institution of Mechanical Engineers, Part O: Journal of Risk and Reliability*, 237(2), 293-313. https://doi.org/10.1177/1748006X211069277

[18] Bolbot, V., Gkerekos, C., Theotokatos, G., Boulougouris, E., 2022. Automatic traffic scenarios generation for autonomous ships collision avoidance system testing. *Ocean Engineering*, 254, 111309. https://doi.org/10.1016/j.oceaneng.2022.111309

[19] Zhu, J., Gao, M., Zhang, A., Hu, Y., Zeng, X., 2022. Multi-ship encounter situation identification and analysis based on AIS data and graph complex network theory. *Journal of Marine Science and Engineering*, 10(10), 1536. https://doi.org/10.3390/jmse10101536

[20] Bakdi, A., Glad, I.K.,Vanem, E., 2021. Testbed scenario design exploiting traffic big data for autonomous ship trials under multiple conflicts with collision/grounding risks and spatio-temporal dependencies. *IEEE Transactions on Intelligent Transportation Systems*, 22(12), 7914-7930. https://doi.org/10.1109/TITS.2021.3095547

[21] Dai, Y., He, Y., Zhao, X., Xu, K., 2024. Testing method of autonomous navigation systems for ships based on virtual-reality integration scenarios. *Ocean Engineering*, 309, 118597. https://doi.org/10.1016/j.oceaneng.2024.118597

[22] Zhu, F., Niu, Y., Wei, M., Du, Y., Zhai, P., 2025. A high-risk test scenario adaptive generation algorithm for ship autonomous collision avoidance decision-making based on Reinforcement Learning. *Ocean Engineering*, 320, 120344. https://doi.org/10.1016/j.oceaneng.2024.120344

[23] Gao, J., Zhang, Y., 2024. Ship collision avoidance decision-making research in coastal waters considering uncertainty of target ships. *Brodogradnja*, 75(2), 75203. https://doi.org/10.21278/brod75203

[24] Zhou, H., Zheng, M., Chu, X., Liu, C., Zhong, C., 2024. Scenario modeling method for collision avoidance testing in inland waterway. *Ocean Engineering*, 298, 117192. https://doi.org/10.1016/j.oceaneng.2024.117192

[25] Mahipala, D., Johansen, T.A., 2024. Smooth scenario-based model predictive control for autonomous collision avoidance in inland waterways. *TechRxiv*. https://doi.org/10.36227/techrxiv.171136997.71159691/v1

[26] Xu, L., Huang, L., Zhao, X., Liu, J., Chen, J., Zhang, K., He, Y., 2025. Navigational decision-making method for wide inland waterways with traffic separation scheme navigation system. *Brodogradnja*, 76(2), 76201. https://doi.org/10.21278/brod76201

[27] Cho, Y., Han, J., Kim, J., 2022. Efficient COLREG-compliant collision avoidance in multi-ship encounter situations. *IEEE Transactions on Intelligent Transportation Systems*, 23(3), 1899-1911. https://doi.org/10.1109/TITS.2020.3029279

[28] Papageorgiou, D., Hansen, P.N., Dittmann, K., Blanke, M., 2022. Anticipation of ship behaviours in multi-vessel scenarios. *Ocean Engineering*, 266, 112777. https://doi.org/10.1016/j.oceaneng.2022.112777

[29] Johansen, T.A., Cristofaro, A., Perez, T., 2016. Ship collision avoidance using scenario-based model predictive control. *IFAC-PapersOnLine*, 49(23), 14-21. https://doi.org/10.1016/j.ifacol.2016.10.315

[30] Hjelmeland, H.W., 2022. Safety validation of marine collision avoidance systems using adaptive stress testing. *Master's thesis*, Norwegian University of Science and Technology (NTNU*)*, Trondheim, Norway.

[31] Weber, R., Sanchez-Heres, L., Sjöblom, T., 2023. COLREG 2: Potential consequences of varying algorithms in traffic situations. *FP7 2022 COLREG 2 Project Report*.

[32] Liu, J., Yang, F., Li, S., Lv, Y., Hu, X., 2024. Testing and evaluation for intelligent navigation of ships: Current status, possible solutions, and challenges. *Ocean Engineering*, 295, 116969. https://doi.org/10.1016/j.oceaneng.2024.116969

[33] Gleeson, J., Dunbabin, M., Ford, J.J., 2024. COLREG scenario classification and compliance evaluation with temporal and multi-vessel awareness for collision avoidance systems. *Ocean Engineering*, 313, 119552. https://doi.org/10.1016/j.oceaneng.2024.119552

[34] Xin, X., Liu, K., Yu, Y., Yang, Z., 2025. Developing robust traffic navigation scenarios for autonomous ship testing: an integrated approach to scenario extraction, characterization, and sampling in complex waters. *Transportation Research Part C: Emerging Technologies*, 178, 105246. https://doi.org/10.1016/j.trc.2025.105246

[35] Ahmed, Y.A., Hannan, M.A., Oraby, M.Y., Maimun, A., 2021. COLREGs compliant fuzzy-based collision avoidance system for multiple ship encounters. *Journal of Marine Science and Engineering*, 9(8), 790. https://doi.org/10.3390/jmse9080790

[36] Namgung, H., Kim, J.-S., 2021. Collision risk inference system for maritime autonomous surface ships using COLREGs rules compliant collision avoidance. *IEEE Access*, 9, 7823-7835. https://doi.org/10.1109/ACCESS.2021.3049238

[37] Fujii, Y., Tanaka, K., 1971. Traffic capacity. *Journal of Navigation*, 24, 543-552. https://doi.org/10.1017/S0373463300022384

[38] Bakdi, A., Glad, I.K., Vanem, E., Engelhardtsen, Ø., 2019. AIS-based multiple vessel collision and grounding risk identification based on adaptive safety domain. *Journal of Marine Science and Engineering*, 8(1), 5. https://doi.org/10.3390/jmse8010005

[39] Namgung, H., 2022. Local route planning for collision avoidance of maritime autonomous surface ships in compliance with COLREGs rules. *Sustainability*, 14, 198. https://doi.org/10.3390/su14010198

[40] Korean maritime safety tribunal (KMST), 2025 Investigation Report. https://kmst.go.kr/eng/board.do?menuIdx=229 (accessed 22nd January 2025)

[41] Korean maritime safety tribunal (KMST), 2025. 'Maritime Accident Statistics'. https://kmst.go.kr/eng/page.do?menuIdx=227 (accessed 19th September 2025)

[42] IMO, 2013. Resolution MEPC.232(65), in: Interim Guidelines for Determining Minimum Propulsion Power to Maintain the Manoeuvrability of Ships in Adverse Conditions.

[43] Cockcroft, A.N., Lameijer, J.N.F., 2011. A Guide to the Collision Avoidance Rules, sixth ed. *Butterworth Heinemann*, Oxford, United Kingdom.

[44] Guidelines for the investigation and adjudication of maritime accidents [effective 12 July 2024] [Korean maritime safety tribunal (KMST) Directive No. 93]. Paragraph. 3. (in Korean), Article 14 (Case Name). https://law.go.kr/admRulSc.do?menuId=5&subMenuId=41&tabMenuId =183&query=%ED%95%B4%EC%96%91%EC%82%AC%EA%B3%A0#J14-0:0 (accessed 19th September 2025)

[45] Lenart, A.S., 2015. Analysis of collision threat parameters and criteria. *Journal of Navigation*, 68, 887-896. https://doi.org/10.1017/S0373463315000223

[46] Busan port navigation rules [effective 1st February 2024] [Busan regional office of oceans and fisheries notice No. 2024-24], Article 17 (Speed Limit) Paragraph 1, [Annex 5] Maximum Navigational Speed (6. New Port Inner Harbor, 7. Gadeok Channel (Inbound/Outbound Fairway) Cautionary Waters) (in Korean). https://law.go.kr/admRulSc.do?menuId=5&subMenuId=41&tabMenuId= 183&query=%EC%84%A0%EB%B0%95%EC%9E%85%EC%B6%9C%ED%95%AD%EB%B2%95#liBgcolor8 (accessed 17th February 2025)

[47] Rezaei, M., 2016. Clustering validation. *PhD dissertation*, School of Computing, University of Eastern Finland, Kuopio, Finland.

[48] Hwang, T., Youn, I.-H., 2021. Navigation situation clustering model of human-operated ships for maritime autonomous surface ship collision avoidance tests. *Journal of Marine Science and Engineering*, 9, 1458. https://doi.org/10.3390/jmse9121458

[49] Taheri, R., Ghahramani, M., Javidan, R., Shojafar, M., Pooranian, Z., Conti, M., 2020. Similarity-based Android malware detection using Hamming distance of static binary features. *Future Generation Computer Systems*, 105, 230-247. https://doi.org/10.1016/j.future.2019.11.034

[50] Lyu, H., Ma, X., Tan, G., Yin, Y., Sun, X., Zhang, L., Kang, X., Song, J., 2024. Identification of complex multi-vessel encounter scenarios and collision avoidance decision modeling for MASSs. *Journal of Marine Science and Engineering*, 12, 1289. https://doi.org/10.3390/jmse12081289

[51] Saraçli, S., Doğan, N., Doğan, İ., 2013. Comparison of hierarchical cluster analysis methods by cophenetic correlation. *Journal of Inequalities and Applications*, 2013, 203. https://doi.org/10.1186/1029-242X-2013-203

[52] Motallebi, H., Nasihatkon, R., Jamshidi, M., 2022. A local mean-based distance measure for spectral clustering. *Pattern Analysis and Applications*, 25, 351-359. https://doi.org/10.1007/s10044-021-01040-5

[53] Sawada, R., Sato, K., Majima, T., 2021. Automatic ship collision avoidance using deep reinforcement learning with LSTM in continuous action spaces. *Journal of Marine Science and Technology*, 26, 509-524. https://doi.org/10.1007/s00773-020-00755-0

[54] Notification on the installation standards and operation of V-pass devices [effective August 30, 2023] [Korea Coast Guard notification No. 2023-10]. (Definition), Article 2. https://law.go.kr/admRulSc.do?menuId=5&subMenuId=41&tabMenuId =183&query=%EC%84%A0%EB%B0%95%ED%8C%A8%EC%8A%A4%EC%9E%A5%EC%B9%98#liBgcolor0, Clause 2 (in Korean) (accessed 19th September 2025)

[55] Amato, F., Fiorini, M., Gallone, S., Golino, G., 2010. e-Navigation and Future Trend in Navigation. *International Journal on Marine Navigation and Safety of Sea Transportation*, 5, 11-14.

[56] Bortuzzo, V., Bertagna, S., Braidotti, L., Bucci, V., 2025. An innovative tool for the evaluation of energy efficiency of merchant ships. *Brodogradnja* 76(3), 76304. https://doi.org/10.21278/brod76304